ELSEVIER

Contents lists available at ScienceDirect

# Science of the Total Environment

journal homepage: www.elsevier.com/locate/scitotenv





# Disruption of boreal lake circulation in response to mid-Holocene warmth; evidence from the varved sediments of Lake Nautajärvi, southern Finland

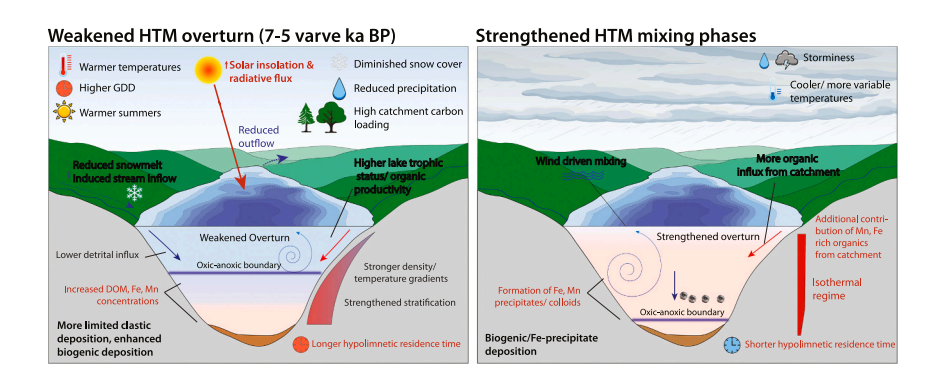
Paul Lincoln<sup>a,\*</sup>, Rik Tjallingii<sup>b</sup>, Emilia Kosonen<sup>c</sup>, Antti Ojala<sup>c,d</sup>, Ashley M. Abrook<sup>e</sup>, Celia Martin-Puertas<sup>a</sup>

- <sup>a</sup> Department of Geography, Royal Holloway University of London, Surrey, UK
- <sup>b</sup> GFZ-German Research Centre for Geosciences. Telegrafenberg, Potsdam D-14473, Germany
- <sup>c</sup> Department of Geography and Geology, University of Turku, Turku, Finland
- <sup>d</sup> Geological Survey of Finland, Espoo, Finland
- e School of Geography and Environmental Science, School of Ocean and Earth Science, University of Southampton, UK

#### HIGHLIGHTS

- 9500 year-long, annually resolved record of Boreal lake mixing responses to different climatic conditions.
- Warmer climates increase organic, Fe and Mn loading, which weakens lake circulation.
- Increased sensitivity to temporary cooling and storminess during warmer periods.
- Holocene Thermal Maximum can act as analogue for lake responses to future climate predictions.

#### GRAPHICAL ABSTRACT



# ARTICLE INFO

Editor: Jay Gan

Keywords:
Lake sediments
Varves
Lake circulation
Holocene thermal maximum

# ABSTRACT

Future climate projections are expected to have a substantial impact on boreal lake circulation regimes. Understanding lake sensitivity to warmer climates is therefore critical for mitigating potential ecological and societal impacts. The Holocene Thermal Maximum (HTM; ca 7–5 ka BP) provides a valuable analogue to investigate lake responses to warmer climates devoid of major anthropogenic influences. Here, we analyse the micro-X-ray core scanning profiles ( $\mu$ -XRF) of the annually laminated (varved) sediments from Lake Nautajärvi (NAU-23) in southern Finland to elucidate changes in lake circulation and sedimentation patterns. Principal component analysis (PCA) identifies two key components in the geochemical data associated with the nature of the sediments, i.e. detrital vs organic sedimentation (PC1), and hypolimnetic oxidation (PC2). Our findings reveal that during the HTM, the lake became more sensitive to changes in oxygenation and mixing intensity. These changes were triggered by a warmer climate, which increased organic matter and redox sensitive metal solute concentrations in the water column, strengthening lake stratification and weakening dimictic circulation patterns. Superimposed on HTM weakened circulation are distinct phases of increased oxidation and iron-rich varve formation that do not happen when the background conditions are cooler (i.e. the early and late

E-mail address: paul.lincoln@rhul.ac.uk (P. Lincoln).

<sup>\*</sup> Corresponding author.

Holocene). This is driven by temporary strengthening of the mixing regime in response to climatic variability and storminess cycles across southern Scandinavia. These findings demonstrate that whilst warmer conditions weaken boreal lake circulation regimes, they can also make them increasingly vulnerable to short term oscillations in prevalent climatic conditions and weather patterns, which could have significant impacts on lake water quality and aquatic ecosystems. These findings underscore the non-stationary nature of lake sensitivity to short-term climatic variability and emphasize the potential for similar shifts to occur under future warming scenarios.

#### 1. Introduction

Future climate projections are expected to have a substantial impact on boreal lakes, with warmer temperatures and longer summer seasons intensifying the thermo-stratification of the water column and altering lake mixing regimes (Shatwell et al., 2019; Woolway and Merchant, 2019; Mesman et al., 2021; Woolway, 2023). This could affect the oxygenation, trophic status and nutrient availability in the lake (Wetzel, 2001; Jansen et al., 2024), and, in turn, have significant impacts on aquatic biodiversity and water quality (Sarkkola et al., 2013; Taipale et al., 2016; Knoll et al., 2018; Krzeminski et al., 2019; Riise et al., 2023).

Presently however, there is limited empirical evidence to confidently predict how boreal lake circulation regimes will respond to warmer climates, which hinders understanding of potential thresholds in lake conditions and the mechanisms that could drive these changes. Analysing the past responses of lakes to warmer climatic conditions, allows us to improve our understanding of natural processes and mitigation strategies for lake ecosystems. The Holocene Thermal Maximum (HTM; ca 7–5 ka BP) is the last pre-industrial period with warmer boreal summers than present (Bova et al., 2021) and thus, provides a valuable analogue to understand boreal lake responses to warmer climatic conditions in the absence of major anthropogenic influences.

Pinpointing the timing, duration and forcing factors responsible for changes in mixing regimes based on sediment records has proven to be a difficult challenge in palaeorecords. This is primarily due to limitations in sampling resolution, chronological precision, and proxy sensitivity to lake circulation (Mishra, 2023). Annually laminated (varved) lake sediments offer a valuable yet underutilised resource for these types of investigations for three reasons. First, varve preservation depends upon seasonally specific sediment yields from the catchment and oxygen concentrations in the water column (Zolitschka et al., 2015). Therefore, variations in varve structure can be used to reconstruct changes in lake circulation and hypolimnetic oxidation (e.g. Dräger et al., 2017; Salminen et al., 2019). Second, the geochemical composition of varved sediments, particularly the profiles of redox sensitive elements (e.g. Fe, Mn and S), can provide information on variations in hypolimnetic oxygenation and circulation regimes over time (e.g. Gälman et al., 2009; Dräger et al., 2016; Zarczyński et al., 2019). Third, precise varve chronologies enable highly-resolved proxy-based reconstruction as well as robust regional comparisons with other well-dated environmental and climatic archives. This can facilitate investigations into whether variations in lake circulation and hypolimnetic oxygenation are responding to local processes or may coincide with climatic variability.

Lake Nautajärvi in southern Finland provides an ideal site to investigate past changes in lake mixing regimes. The sedimentary record is continuously varved for the past 9900 years, indicating persistent seasonal hypoxia in the hypolimnion throughout the Holocene (Ojala and Alenius, 2005). Furthermore, the occasional occurrence of Fe and Mn precipitates identified within the sediment sequence suggests subtle variability in lake sedimentation patterns (Ojala et al., 2013), potentially linked to seasonal changes in hypolimnetic lake oxygen status and mixing (e.g. Gälman et al., 2009; Neugebauer et al., 2022; Żarczyński et al., 2022). Therefore, the Nautajärvi sediment sequence provides the opportunity to investigate changes in lake oxygenation and circulation, and possible forcing factors, at a seasonal to annual resolution. By using the Nautajärvi varved sequence, this study aims to improve our

understanding of lake circulation and sedimentation patterns through the warmer climatic regimes of the HTM. Specifically, it seeks to (i) characterize variability of lake circulation using sediment varve parameters and  $\mu$ -XRF core scanning data; (ii) evaluate the potential causes (catchment-to-lake processes) of changes in lake circulation dynamics through the HTM; and (iii) provide insights for future warming scenarios by considering how circulation dynamics recorded at Nautajärvi, may inform predictions on boreal lake responses to future warming.

# 2. Site description

Nautajärvi ( $61^{\circ}48'N$   $24^{\circ}24'E$ ) is a small ( $0.17 \text{ km}^2$ ) seasonally stratified, 20 m deep, mesotrophic and slightly acidic (pH  $\sim$ 5.8–6) lake (Korkonen et al., 2017) in southern Finland (Fig. 1). The lake lies at 103.7 m asl and sits in a chain of lakes within the larger-scale drainage basin of Äväntäjärvi (Fig. 1A). The lake was formed after the Early Holocene recession of the Fennoscandian Ice sheet and the subsequent isolation from the Baltic Sea basin via glacioisostatic uplift, during the Lake Ancylus phase at 9625 varve yr BP (equivalent to varve chronology years before 1950 CE; Ojala et al., 2005).

The lake is fed by the adjacent Ristijärvi located to the north, and two streams draining the surrounding catchment, which consists of coarse-grained granites, till and post-glacial silts (Ojala and Alenius, 2005). The only outflow drains into Lake Pitkävesi to the south. Vegetation in the catchment area is dominated by pine and spruce trees characteristic of the Southern boreal vegetation zone. The contemporary local climate, recorded at the Halli weather station 8 km NE of the lake, is continental, with mean annual precipitation ranging between 500 and 700 mm between 1990 and 2011, of which approximately 30 % falls as snow (Jokinen et al., 2021). Mean annual temperatures are +4 °C, with the warmest temperatures occurring in July (+15–22 °C) and the coldest temperatures occurring between January to February (-12 to -4 °C). Typically, the lake is ice covered for 4–5 months a year, from mid-December until mid-May (Figs. 1 C-E).

# 2.1. Present lake mixing and sedimentation regimes

Limnological measurements by the Finnish Environment Institute (OIVA database, <a href="https://www.syke.fi/en-US/Open\_information">https://www.syke.fi/en-US/Open\_information</a>) and sediment trap surveys by Ojala et al. (2013) and Korkonen et al. (2017) show that the contemporary circulation regime at Nautajärvi is dimictic (i.e. two overturn periods annually). The first overturn occurs in spring, as winter ice cover melts, the lake surface is subaerially exposed, and the water column becomes isothermal. During summer, warmer temperatures induce thermal stratification, which is maintained until autumn, when cooling lake surface temperatures and increased precipitation, winds and storms promote a second overturn. In winter, the lake is ice covered and inversely stratified, and the hypolimnion is anoxic. The preservation of varves indicates the absence of *in situ* sediment mixing by bioturbation, likely caused by the dimictic nature of the lake, where anoxia prevails at the sediment-water interface during periods of winter ice-cover and summer stratification.

The sedimentary sequence in the centre of Nautajärvi is composed of clastic-biogenic varves, which are typical of Holocene boreal lakes across Fennoscandia (e.g. Renberg, 1981; Ojala and Alenius, 2005; Zolitschka et al., 2015). The varves consist of two primary laminae, which represent the lake circulation and seasonal sedimentation

dynamics described above (Ojala et al., 2013). A detrital-rich lamina is composed of normally graded felspars, quartz-rich minerals and biogenic silica from the catchment, which is primarily controlled by winter snow storage and discharge intensity following spring snowmelt (Ojala and Alenius, 2005; Ojala et al., 2013; Korkonen et al., 2017). An organic-rich layer composed of amorphous organic material is controlled by in-lake productivity and allochthonous transport from inflowing streams in summer (Ojala et al., 2013; Saarni et al., 2016).

#### 3. Methodology

To investigate the changes in lake sedimentation and circulation regime, we use new cores collected from the deepest section of Nautajärvi in March 2023 (NAU-23), using a gravity piston corer from the frozen lake surface. A 7.26 m composite NAU-23 stratigraphy was

constructed using 10 drives from 4 cores spaced <10 m apart (A to D, Fig. 1). The Nautajärvi sediment chronology is based on semi-automated varve counting and measurements of seasonal laminae variations (Ojala and Tiljander, 2003). The accuracy of the varve chronology was estimated as  $\pm 1$ % based on replicated varve analyses of multiple sediment cores (Ojala and Alenius, 2005). The varve chronology was crosschecked by comparing palaeomagnetic measurements with other independently varve-dated palaeomagnetic records from Finland (Ojala and Tiljander, 2003) and Sweden (Snowball et al., 2007).

Here, the varve chronology was transferred to the NAU-23 stratigraphy using linear interpolation between 210 marker layers between -46 and 9829 varve yr BP (Ojala and Alenius, 2005; Supplementary Fig. 1).

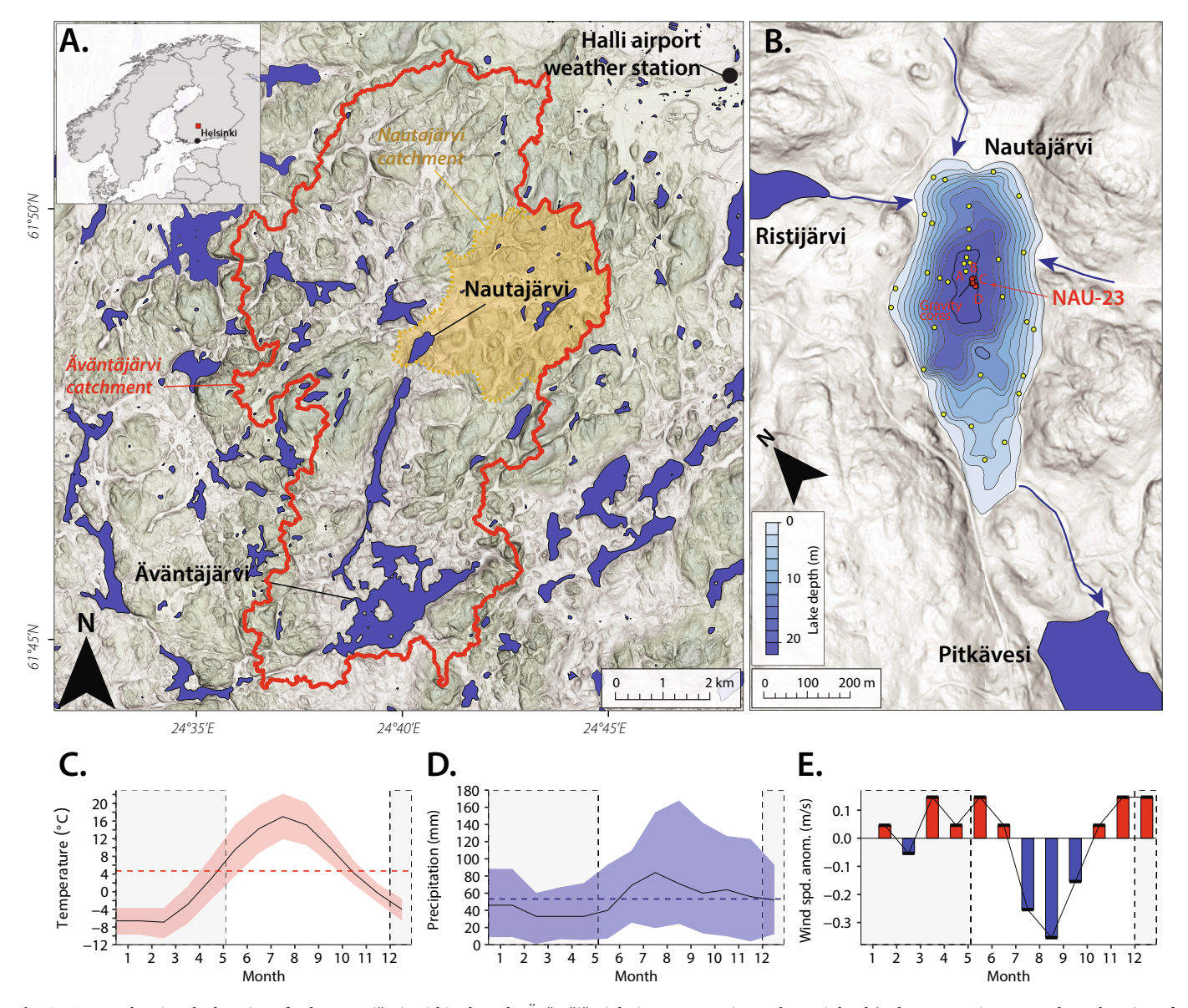


Fig. 1. A. Map showing the location of Lake Nautajärvi, within the Lake Äväntäjärvi drainage system in southern Finland (red square on inset map shows location of Äväntäjärvi catchment). The extent of the Äväntäjärvi catchment is in red and the Nautajärvi catchment is in dark yellow. The Digital Elevation Model is a 2m resolution product obtained from the National Land Survey of Finland Topographic Database 06/2014. B. Shows the lake bathymetry and coring locations for the NAU-23 sequence (in red). Yellow dots show cores previously extracted from the lake. Lake inflows and outflows are marked by blue arrows. C-E. Mean monthly temperature (C.), precipitation (D.), and wind speed (E. plotted as monthly anomalies from the annual mean) between 1990 and 2011, derived from the Halli weather station ~8 km NE of the lake (position shown in 1A; Jokinen et al., 2021). Red and blue ribbons show the monthly temperature, and precipitation ranges, whilst horizontal dotted lines show annual mean values. In E., red and blue bars represent positive and negative anomalies from the annual mean. Grey rectangles show the average duration of lake ice cover between December and May (Korkonen et al., 2017)

#### 3.1. *u-XRF* core scanning

Geochemical element profiles of the NAU-23 cores have been acquired directly at the split-core surface every 0.2 mm using an ITRAX  $\mu\text{-XRF}$  core scanner at GFZ-Potsdam. All cores were measured continuously and additionally, 2 to 3 selected intervals of about 2 cm long were selected to obtain replicate measurements.  $\mu\text{-XRF}$  core scanning measurements were conducted using a dwell time of 6 s, with an Rh-X-ray source operated at 30 kV and 60 mA. This covers the elements Aluminium (Al) through to Zircon (Zr) as well as the coherent (Rh coh) and incoherent (Rh inc) radiation. The elements Si, S, K, Ca, Ti, Mn and Fe were selected for further investigations based on the relative standard deviations (<25 %) calculated from 3-fold replicate measurements.

Element records acquired by  $\mu$ -XRF core scanning are typically expressed as intensities (cps) that are non-linearly related with element concentrations due to sediment matrix effects, but also influenced by physical sediment properties (Tjallingii et al., 2007; Weltje and Tjallingii, 2008). However, log-ratios of element intensities are linear functions of element concentrations (Weltje et al., 2015), and also provide a solution for statistical analyses of compositional data (Aitchison, 1986).

Element intensities were first resampled to 0.4 mm resolution and then transformed using a centered-log ratio (clr) in the 'composition' R package (van den Boogaart and Tolosana-Delgado, 2008), to account for constant-sum constraints (Aitchison, 1986), and non-linear behaviour to variations in the geochemical composition of the sediments (Tjallingii et al., 2007).

Statistical analyses were undertaken using R version 4.3.3. Element values were scaled using the replicate variance measurements, to downweight elements with low analytical precision (Weltje et al., 2015). Ward's hierarchical clustering, used to statistically group and interpret trends in the multivariate dataset, was performed on the clr-transformed and scaled  $\mu$ -XRF data using the 'stats' and 'dendextend' packages (Galili, 2015).

The relevant number of clusters (k=4) was selected using the majority rule from 26 indices run using 'NBClust', manually constrained to between 4 and 10 possible clusters (Charrad et al., 2014; Supplementary Data), and visualised using the 'ComplexHeatmap' package (Gu and Hübschmann, 2022).

Principal component analysis (PCA), used to identify key trends in the multivariate data, were performed using the 'FactoMineR' package (Lê et al., 2008) and visualised using 'factoextra' (Kassambara and Mundt, 2017) and 'ggplot2' (Wickham, 2016). Other statistical analyses were undertaken using 'corrplot' (Wei et al., 2017) and 'zoo' (Zeileis et al., 2023). The code used to undertake these analyses are included in the Supplementary Data.

# 3.2. Microanalysis with SEM

A Jeol JSM-5900 low vacuum scanning electron microscope (SEM) connected to an Oxford Instruments X-Max 80mm<sup>2</sup> energy-dispersive spectrometer (EDS) was used to investigate sections of anomalously high values of iron (Fe) and manganese (Mn) in the sequence. The analyses were done on carbon coated epoxy embedded samples (Tiljander et al., 2002). Here, the backscattered electron image (BSEI) mode was used for detailed studies of micro sedimentology, composition and structure of varves, as well as spatial distribution and composition of Fe and Mn precipitates seen in the sediment sequence (e.g. Ojala and Francus, 2002).

# 4. Results

4.1. Sediment description and correlation to the Nautajärvi varve chronology

The NAU-23 sedimentary sequence consists of two units as described

by Ojala and Alenius (2005). Unit 1 is at the base of the sequence between 726 and 674 cm (Lake Ancylus phase; Fig. 2) and is made of massive to faintly laminated minerogenic clayey-silts, with irregularly spaced fine-medium sand beds. Unit 2 covers the rest of the record and is comprised of clastic and biogenic laminae forming the varve couplets (674–0 cm).

Whilst the varve model does not change over time, the varves at the base of unit 2 (674–630.5 cm; 9829–9625 varve yr BP) are thicker (2.39  $\pm$  1.24 $\sigma$  mm) because of a higher amount of clastic input into the lake, before grading into thinner (0.62  $\pm$  0.24 $\sigma$  mm) clastic-biogenic varve couplets after isolation from Lake Ancylus at 9625  $\pm$  96 varve yr BP (Ojala et al., 2005). From 432 to 310 cm of sediment depth (7000–5000 varve yr BP), the varves are frequently iron stained and contain beds of concentrated Fe-rich precipitates and colloids (Fig. 3A). Fe precipitates are spherical in shape and typically <5  $\mu$ m in diameter (ranging between 1 and 15  $\mu$ m; colloids hereafter). They seem to concentrate more in the organic lamina of the varve, although when appearing in abundance, they are spread throughout the two varve laminae. SEM EDS analysis shows that the colloids consist of 85–93 % Fe, 7–9 % Mn and residual Ca (2–2.5 %) and P (3–4 %) (Fig. 3B; Table 1).

Whilst these types of precipitate have previously been recorded in Fennoscandian varves (e.g. Anthony, 1977; Renberg, 1981; Ballo et al., 2023), the occurrence of clastic laminae within the varve couplets (Fig. 3B; Fig. S2) demonstrates that the clastic-biogenic mode of varve formation was persistent at Nautajärvi, despite enhanced iron and manganese precipitation (section 2.1). Prominent iron staining and colloid preservation is only prevalent between 432 and 310 cm and not elsewhere in the stratigraphy, and macroscopic changes in the rest of the varves reflects the relative contribution of the clastic and biogenic laminae to the total varve thickness.

# 4.2. Elemental composition of the sediments

The high-resolution  $\mu\text{-}XRF$  data enables further investigations into the geochemical composition of the NAU-23 varved sediments (Fig. 2). Trends in the multivariate geochemical data are typically interpreted using hierarchical clustering (Fig. 4A) and PCAs (Fig. 4B-C). For the  $\mu\text{-}XRF$  core-scanning data of the entire varved NAU-23 sequence (n=18,125), principal components 1 and 2 (PC1–2) explain 78.8 % and 11.7 % of the data variance respectively (Fig. 4B). Additional statistical data and PCA results from individual clusters are included in the supplementary information (Fig. S5).

The major positive contributors to variability in PC1 are the lithogenic elements Ti<sub>clr</sub>, K<sub>clr</sub>, Ca<sub>clr</sub> and Si<sub>clr</sub>, (loadings ≥0.35; Fig. 4B-C) whilst redox-sensitive elements Feclr, Mnclr and Sclr are weak negative contributors (-0.01 to -0.25). The strongest positive loadings on PC axis 2 are the redox sensitive elements  $Fe_{clr}$  and  $Mn_{clr}$  (0.59 and 0.70 respectively), whilst  $S_{\text{clr}}$  is the most strongly negatively loaded element (-0.25). The lithogenic elements are weakly positively loaded on PC2 (<0.25). Comparisons of PC1 axis values to the varve structure in the uppermost section of the NAU-23 sequence (6-0 cm) shows that the highest values are most closely associated to the clastic laminae, whilst the lowest values align with the biogenic laminae (Fig. 4D). The sub annual pattern is less clear for PC2 due to lower inter-sample variance through this section of the sequence. Positive loading of Feclr and Mnclr on PC2 and negative loading on PC1 however, supports that PC2 peaks are more closely associated with the biogenic, rather than the clastic laminae. This is consistent with the previous lake monitoring survey, where Fe and Mn precipitates were observed in the water column primarily during the autumn and winter months (Ojala et al., 2013).

Ward's hierarchical clustering was used to statistically group core sections with similar geochemical compositions (Fig. 4A). The four hierarchical clusters are clearly distributed along PC1 (Fig. 4B). The most negative PC1 values, reflecting sedimentation most weakly dominated by the lithogenic elements, are associated with cluster 1 (red). Slightly negative to slightly positive PC1 values are associated with cluster 2

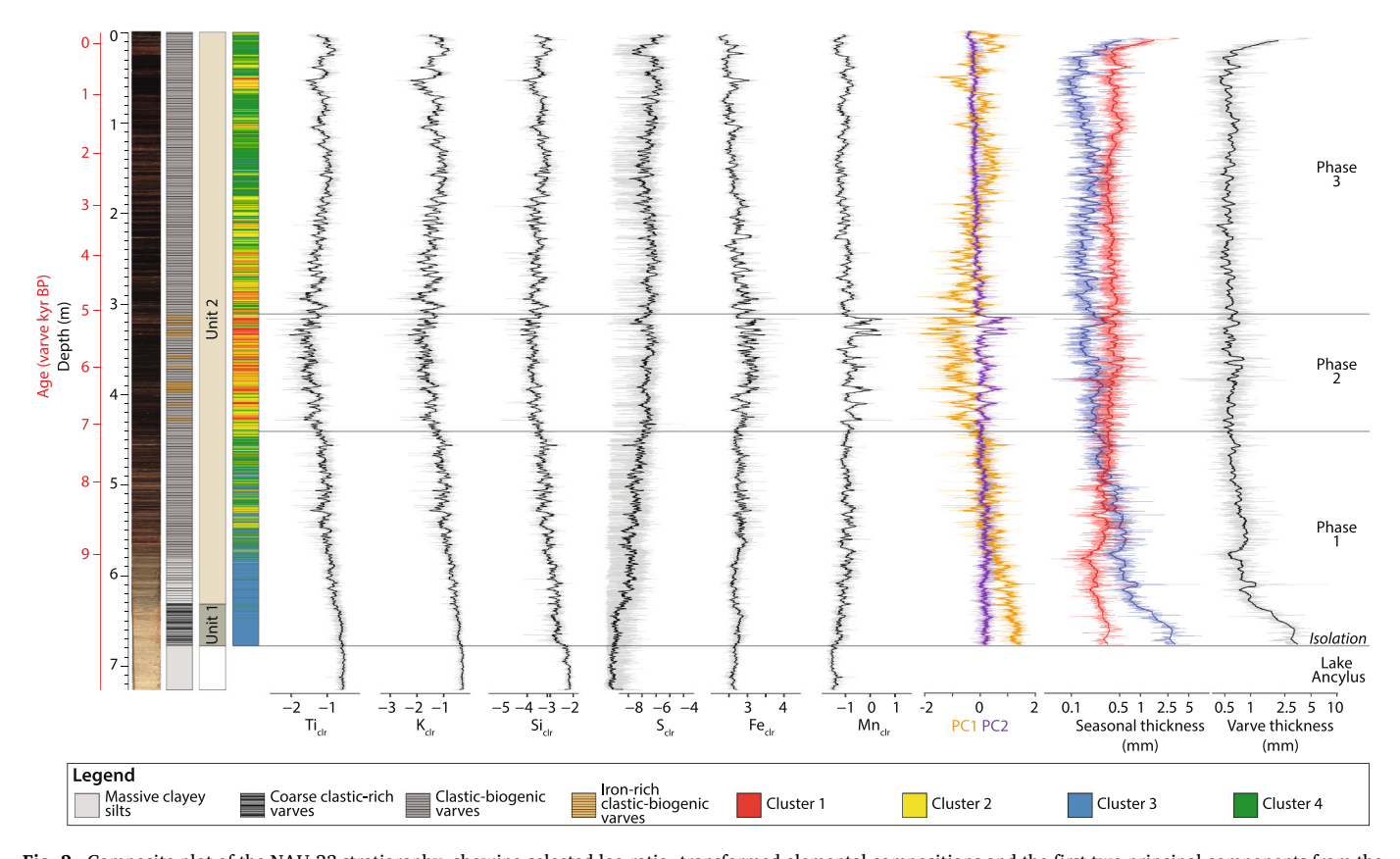


Fig. 2. Composite plot of the NAU-23 stratigraphy, showing selected log ratio -transformed elemental compositions and the first two principal components from the PCA analysis (PC1 in orange, PC2 in purple). The two units in the varve stratigraphy (unit 1 and unit 2) are also highlighted. Lighter lines are the 0.4 mm resolution μ-XRF data and the darker lines are a 25-point moving average (equivalent to 10 mm). The distribution of the Ward's hierarchical clusters (section 4.2) are plotted next to the sediment stratigraphy, and the first two principal components from the PCA analysis. Log transformed annual (black), summer (red) and winter (blue) varve thicknesses) from Ojala and Alenius (2005) are also plotted to illustrate comparable trends to the geochemical data. Thick black, red and blue curves in these plots are 50 yr moving averages.

(yellow) and cluster 4 (green), respectively. The most positive PC1 values, reflecting sedimentation most strongly dominated by the lithogenic elements are associated with cluster 3 (blue). The most positive PC2 values (>1) are contained entirely within cluster 1 at the most negative end of the PC1 scale (Fig. 4B).

According to the stratigraphical position of the clusters and the PC axis values, the varved sequence (unit 2) can be divided into three phases (Fig. 2).

# 4.2.1. Phase 1 (674-432 cm; 9829-7000 varve yr BP)

PC1 values are initially high (>1 prior to ~9000 varve yr BP), before steadily declining (to <0) between 9000 and 7000 varve yr BP (mean =  $0.54 \pm 0.53\sigma$ ). This coincides with the replacement of cluster 3 into cluster 4 (50.32 % and 33.69 % of the total Phase 1 clusters respectively). PC2 values show limited variability, oscillating between -0.1 and 0.5 (mean =  $0.15 \pm 0.20\sigma$ ). Sedimentologically, this phase records the transition from thick varves ( $2.26 \pm 1.24\sigma$  mm > 9600 varve yr BP), dominated by the clastic laminae, to progressively thinner clastic-biogenic varves ( $0.73 \pm 0.26\sigma$  mm between 9600 and 7000 varve yr BP), with progressively increasing organic laminae thicknesses.

# 4.2.2. Phase 2 (432–310 cm; 7000–5000 varve yr BP)

PC1 values are the lowest in the entire sequence (mean  $=-0.71\pm0.53\sigma$ ), coinciding with thinner varves couplets (average varve thickness of  $0.60\pm0.20\sigma$  mm). PC2 values however, show a higher variance than Phase 1, oscillating between -0.3 and 2.1 (mean  $=0.50\pm0.31\sigma$ ). Cluster 1 and cluster 2 are the most dominant clusters in Phase 2 (37.68 % and 51.04 % of the total Phase 2 clusters respectively), reflecting reduced lithogenic element concentrations and higher biogenic varve

thicknesses. Samples assigned to cluster 1 are closely aligned with the highest PC2 peaks (>1) and coincide with the occurrence of Feprecipitates in the varves at  $\sim$ 6910–6790, 6660–6560, 6405–6290, 6250–6080,5980–5950, 5850–5810, 5430–5380, 5350–5280 and 5230–5100 varve yr BP (Fig. 3).

# 4.2.3. Phase 3 (310-0 cm; 5000 varve yr BP to present)

PC1 values are higher than Phase 2 (mean  $=-0.14\pm0.50\sigma$ ), increasing from -1 to >1 between 5000 and 2000 varve yr BP, and then oscillating between -1.6 and 1.5 through the rest of the sequence (2000-72 varve yr BP). Increases in PC1 reflects sedimentological changes observed in the varves, where an increase in the thickness of the clastic laminae is also observed (average varve thickness of  $0.57\pm0.23\sigma$  mm). PC2 values return to more stable variability (mean  $=-0.18\pm0.16\sigma$ ). The modal clusters of Phase 3 are cluster 2 and cluster 4 (35.26 % and 55.90 % respectively), coinciding with the higher PC1 values and increased clastic laminae thicknesses during the mid-late Holocene (5000- -72 varve yr BP).

# 5. Interpretation of the NAU-23 principal components

# 5.1. PC1- a proxy for detrital-biogenic sedimentation

The strong loading of lithogenic elements on PC1 and comparable trends to the clastic laminae thicknesses, indicates a close association with detrital sedimentation into the lake. Ti and K in particular, are reliable proxies for allogenic sedimentation from the catchment as they are insensitive to biogenic processes operating within the lake water (Bertrand et al., 2023). Ca<sub>clr</sub> and Si<sub>clr</sub> however can be derived from

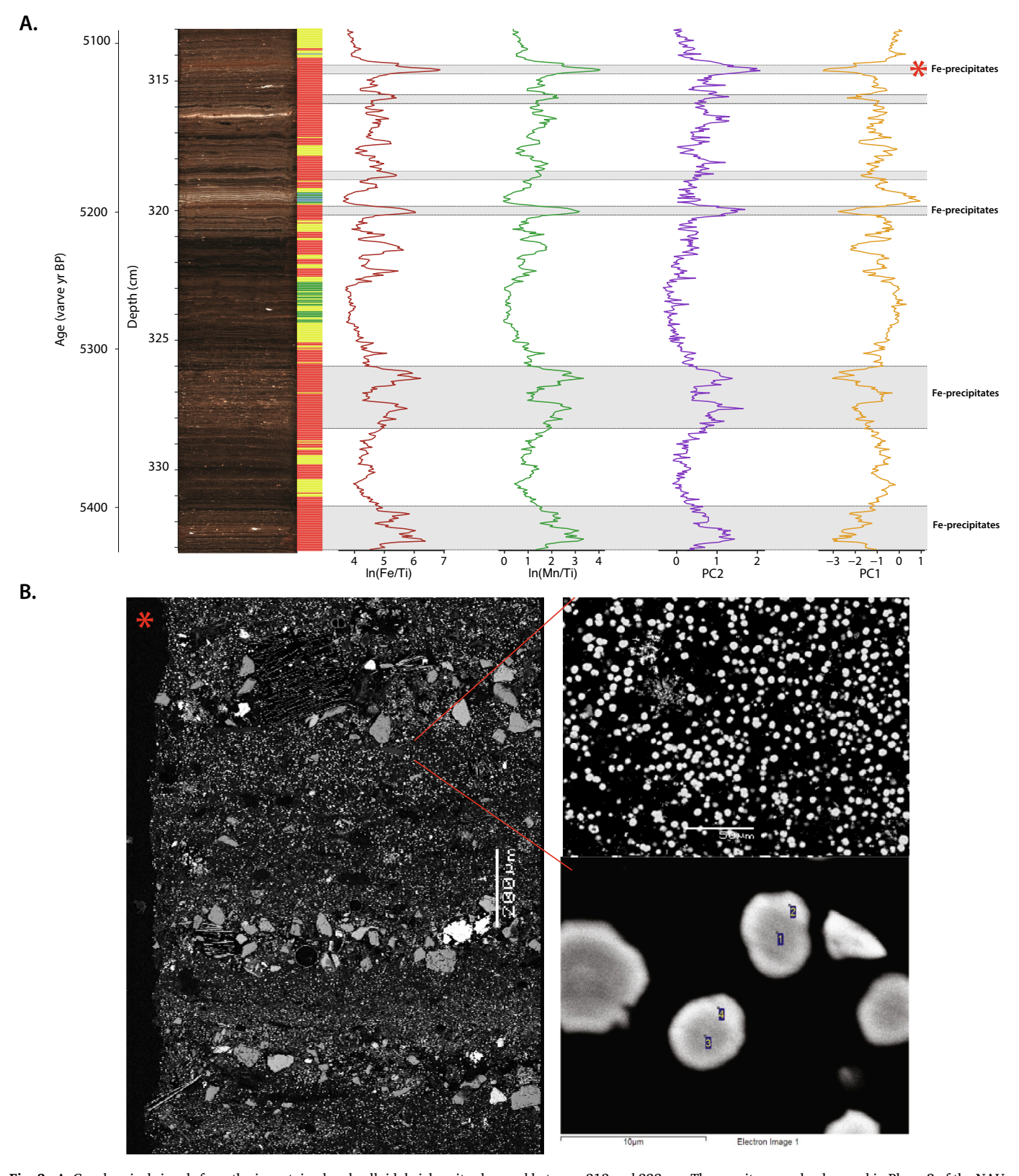


Fig. 3. A. Geochemical signals from the iron stained and colloidal-rich units observed between 313 and 333 cm. These units are only observed in Phase 2 of the NAU-23 sequence between ca 7000 and 5000 varve yr BP. Grey bands show the locations of iron-rich laminae. Cluster colours shown alongside the core image follow Fig. 2. B. SEM EDS images (left-hand side) of the brown iron stained and colloid-rich units between 314 and 315 cm (ca 5200 varve yr BP) (location marked by a red star in A). Greyscale images on the right-hand side shows that the dense (white) spherical colloids/precipitates are present throughout the varve year, although angular clastic particles within clastic-rich laminations characteristic of the spring minerogenic layer are still preserved. Geochemical analysis undertaken on the clastic layer is included in Fig. S2.

Table 1
Geochemical analysis of the colloidal material, confirming that they are principally composed of Fe and Mn. The position of these samples is shown in Fig. 3B.

Sample	P (%)	Ca (%)	Mn (%)	Fe (%)	Total (%)
1	3.31	2.29	8.60	85.90	100
2	4.33	2.27	7.97	85.42	100
3			7.80	92.20	100
4	3.98		7.94	88.08	100
Max	4.33	2.27	8.60	92.20	
Min	3.31	2.20	7.80	85.42	

authigenic as well as allogenic sources, most notably via Si-rich diatom blooms (Ojala et al., 2013), which would be expected to contribute to the Si content of the sediment. The strong positive correlations between Si\_{clr} and Ca\_{clr} to Ti\_{clr} ( $r \geq 0.85$ ,  $p \leq 0.05$ ; Fig. S3), and positive loadings on the PC1 axis, however, show that these elements are derived principally from allogenic rather than authigenic sources. PC1 is therefore interpreted to reflect relative shifts in detrital and organic sedimentation in the lake, with higher values indicating more allogenic sedimentation of clastic material transported from the lake catchment, principally during the spring melt season, and lower values reflecting more authigenic sedimentation of organic material through the growing season and

winter months.

#### 5.2. PC2- a proxy for hypolimnetic oxidation

The three most strongly loaded elements associated with PC2 (Fe  $_{
m clr}$ , Mn  $_{
m clr}$ , S $_{
m clr}$ ) are all redox-sensitive, and can also accumulate in lakes via several different processes. These include detrital and organic influx, and syn- and post-sedimentary diagenetic processes driven by changes in redox conditions within the water column and sediments (e.g. Davison et al., 1982; Gälman et al., 2009; Żarczyński et al., 2019; Makri et al., 2021).

Weak loading on PC1 (Fig. 4B-C) shows that direct allogenic sources are not the major contributors to Fe and Mn accumulation, and consequently, variability in PC2 values. This is supported by two lines of evidence. First, comparable trends observed between PC2 and Fe and Mn normalised with respect to Ti (ln(Fe/Ti) and ln(Mn/Ti); Fig. 3A), suggest that variability in PC2 is consistent with shifts in authigenic Fe and Mn concentrations. Second,  $S_{\rm clr}$ , which is sensitive to changes in redox conditions but in the opposite direction to Fe and Mn, is negatively loaded on PC2. Under anoxic conditions Fe and Mn exist as soluble reduced ions (Fe<sup>2+</sup> and Mn<sup>2+</sup>), but in the presence of oxygen, they oxidize and precipitate as insoluble hydroxides or oxides (Davison, 1993). In contrast, S exists as stable, soluble sulphate ions (SO<sub>4</sub><sup>2-</sup>) in

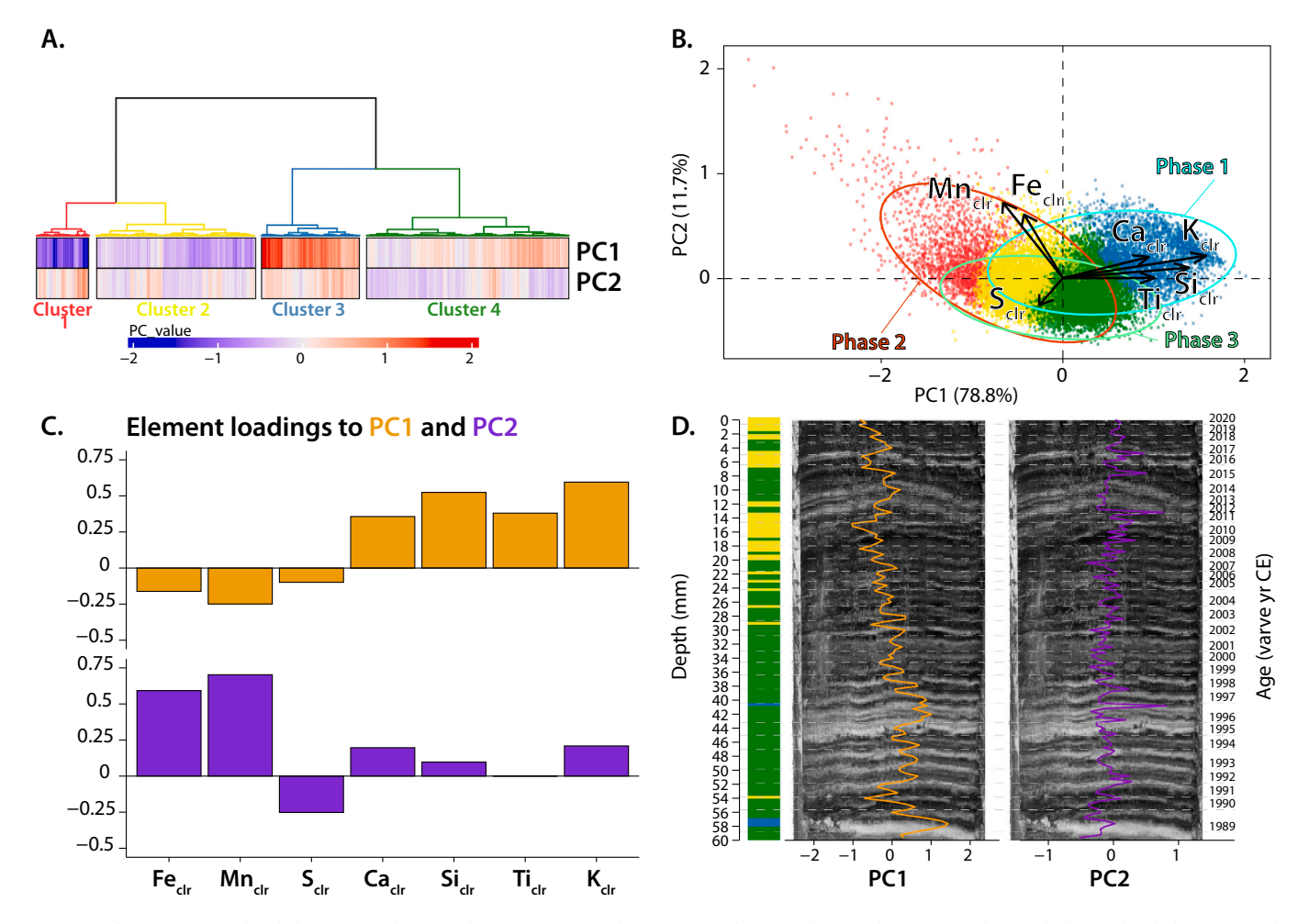


Fig. 4. Results of the hierarchical clustering and PCA of the NAU-23  $\mu$ -XRF dataset. A. Dendrogram showing the results of the Ward's hierarchical clustering of the NAU-23 sequence. Heatmaps show the ranges of PC1 and PC2 values associated with each cluster. B. Principal component analysis (PCA) biplot of the  $\mu$ -XRF geochemical data through the varved section of the NAU-23 sequence. Values are coloured with respect to the hierarchical clustering shown in 4A. The ellipses represent the 99 % ranges of Phases 1–3 discussed in the manuscript. C. Loadings of the elements to PC1 and PC2. D. Depth profiles from the surface core of the NAU-23 covering the last 31 years. The grey-scaled core photo in combination with down-core variations of the clusters (left), PC1 and PC2 reveal variations in response to the clastic (light) and biogenic (dark) varve structure. Cluster values (modally clusters 2 and 3) following the colour scheme of 3A are plotted alongside the surface cores.

oxic conditions, while sulphate-reducing bacteria convert sulphates to form insoluble sulphides under enhanced anoxia ( $S^{2-}$ ; Luo, 2018). Therefore, we conclude that the formation, transportation and deposition of Fe, Mn and S precipitates, and consequently variability in PC2, is primarily controlled by redox processes.

Fe and Mn solubility is sensitive to redox at different rates and redox potentials (Makri et al., 2021), whereby Mn ions are more sensitive to shifts from anoxic to oxic conditions than Fe. This rationale is regularly used to justify the ln(Fe/Mn) ratio as a proxy for hypolimnetic redox variations (e.g. Naeher et al., 2013). We refrain from this interpretation for two reasons. First, persistent hypolimnetic hypoxia at Nautajärvi promotes the diagenetic formation of Fe and Mn, which would impact the ln(Fe/Mn) ratio sensitivity to redox conditions (Makri et al., 2021). Second, the Fe-rich catchment bedrock means that although the PCA analyses suggest a negligible contribution of detrital sources, the allogenic influx of redox sensitive elements, particularly via soil and wetland contributions, cannot be discounted entirely. Whilst this does not invalidate that the concentration of these elements are indicative of benthic hypoxia, it does suggest that it is not the only factor affecting Mn and Fe concentrations and consequently the ln(Fe/Mn) ratio.

The redox sensitivity of the dominant elements contributing towards PC2, supports that this axis represents changes in the oxidation state of the water column, which in turn reflects the mixing intensity and hypolimnetic oxygenation status during the spring and/or autumn months (e.g. Żarczyński et al., 2022; Ballo et al., 2023). Higher PC2 values indicate increased Fe and Mn precipitation during overturn intervals. During these periods, the redox boundary in the water column lowers into the hypolimnion, allowing Fe and Mn-rich waters to upwell. This catalyses the oxidation and precipitation of the metal solutes into soluble forms, which are then incorporated into the sediment via rainout. In turn, lower values reflect reduced Fe and Mn accumulation, either during phases of less vigorous overturning and disturbance of the hypolimnetic waters, or reduced Fe and Mn concentrations in the hypolimnion.

The negative correlations between  $Fe_{clr}$  and  $Mn_{clr}$  to  $S_{clr}$  also provides an indication of the strength of anoxia maintained in the hypolimnion. Sulphate reduction, which requires lower redox potentials than the oxidation of Fe and Mn (Algeo and Li, 2020), leads to the formation of iron sulphides (e.g., FeS) under anoxic conditions. The negative correlation of  $Fe_{clr}$  and  $S_{clr}$  throughout the NAU-23 sequence (Fig. S5), suggests that the strongly reducing conditions required to form FeS precipitates were not maintained throughout the annual cycle. Therefore, we conclude that whilst the lake mixing cycles were either not deep enough or too short to substantially impact the sediment-water interface, they were able to recycle dissolved oxygen into the hypolimnion and prevent persistent anoxia.

The use of PC2 values as a stable proxy of hypolimnetic mixing regimes is dependent on consistent abundances of reduced Fe and Mn ions in the hypolimnion. This is unlikely, as dissolved Fe and Mn concentrations are presumed to have varied substantially through the Holocene in response to factors including catchment vegetation, lake trophic status and residence time. Consequently therefore, PC2 is interpreted as a relative/ non-stationary proxy for hypolimnetic hypoxia, subject to dissolved Fe, Mn and S concentrations in the lake water. This is supported by the hierarchical clustering results where the most positive PC2 values (>1), coinciding with iron-rich varves, are contained entirely within cluster 1, at the most negative end of PC1 (Fig. 4B). This demonstrates that there is a close positive association between organic-rich varve deposition, enhanced Fe and Mn accumulation and colloidal precipitation.

# 6. Nautajärvi in the context of regional climatic and environmental change

The sedimentology and geochemical analyses of the NAU-23 sequence provides a detailed framework for understanding the

sedimentation dynamics and lake mixing regimes. The lake record is divided into three distinct phases (defined in section 4.2), each corresponding to significant shifts in either landscape conditions or regional climate.

# 6.1. Phase 1- catchment configuration during the early to mid-Holocene transition (9829–7000 varve yr BP)

Varve formation was initiated in Nautajärvi at 9829  $\pm$  98 varve yr BP, before the lake became isolated from Lake Ancylus (Ojala et al., 2005), and the internal morphometry and sheltered surrounding topography of the basin induced hypolimnetic hypoxia (Ojala et al., 2000). Between 9500 and 7000 varve yr BP, decreasing PC1 values align with trends in clastic varve thickness, suggesting reduced snowmeltderived clastic influx and increased biogenic productivity during the growing season (Fig. 5). Detrital material was primarily sourced from the fluvial inflows, which were fed by large volumes of available water locked up as snow. Low vegetation cover, particularly soon after lake isolation, also facilitated erosion of the unconsolidated glacigenic and marine sediments outcropping on the catchment slopes. This contributed to the thicker clastic laminae and a predominance of cluster 3 at the base of the NAU-23 sequence. These trends all follow the lagged millennial scale climatic amelioration signals, and a lengthening of the growing season recorded in palynological records across southern Scandinavia in the Early Holocene (Seppä et al., 2009; Sejrup et al., 2016). Together, this invokes a steady shift in dominant seasonality, with a decreasing (increasing) winter (growing season) contribution to the annual sedimentation (Fig. 5). We attribute the limited variability in PC2 through Phase 1 to the lower growing season contribution to annual sedimentation, alongside lower vegetation densities and juvenile soil and peatlands, which limited allogenic organic and ferric influx (Ojala and Alenius, 2005).

# 6.2. Phase 2- the Holocene thermal maximum (HTM; 7000–5000 varve yr BP)

The PC1 and PC2 trends in Phase 2 align with increases in Fe, Mn, dissolved organic matter (DOM), and lake trophic status through the HTM. These trends are also reflected in the seasonal varve laminae, where thinner detrital laminae and thicker organic laminae indicate sedimentation driven primarily by authigenic productivity during the growing season, with minimal allogenic clastic input (Fig. 5). This suggests reduced catchment erosion, likely tied to decreases in winter snow accumulation and/or shorter periods of winter lake ice cover (Ojala and Alenius, 2005). Together, these observations point to seasonally warm and dry conditions in southern Finland, with warm, extended summers and mild winters (Tiljander et al., 2003; Haltia-Hovi et al., 2007).

This is consistent with high mean annual and summer temperatures and increased growing degree days >5 °C (GDD), recorded across boreal European latitudes during the HTM (e.g., Heikkilä and Seppä, 2003; Ojala et al., 2008; Borzenkova et al., 2015; Engels, 2021; Wastegård, 2022; Salonen et al., 2024). Although warm climates persisted throughout the year, they were particularly focused into the summer months, when temperatures in southern Scandinavia were 2.5–3.5 °C warmer than present (Borzenkova et al., 2015).

Whilst warmer and drier conditions would cause a net increase in evaporation at the lake surface, the extensive and interconnected nature of the lake chains within the Äväntäjärvi drainage basin suggests that lake-levels at Nautajärvi were unlikely to have been significantly lower during the HTM. This is supported by contemporary lake-level observations in the vicinity of Nautajärvi, which decrease by only 10–30 cm during to historic drought periods (Veijalainen et al., 2019).

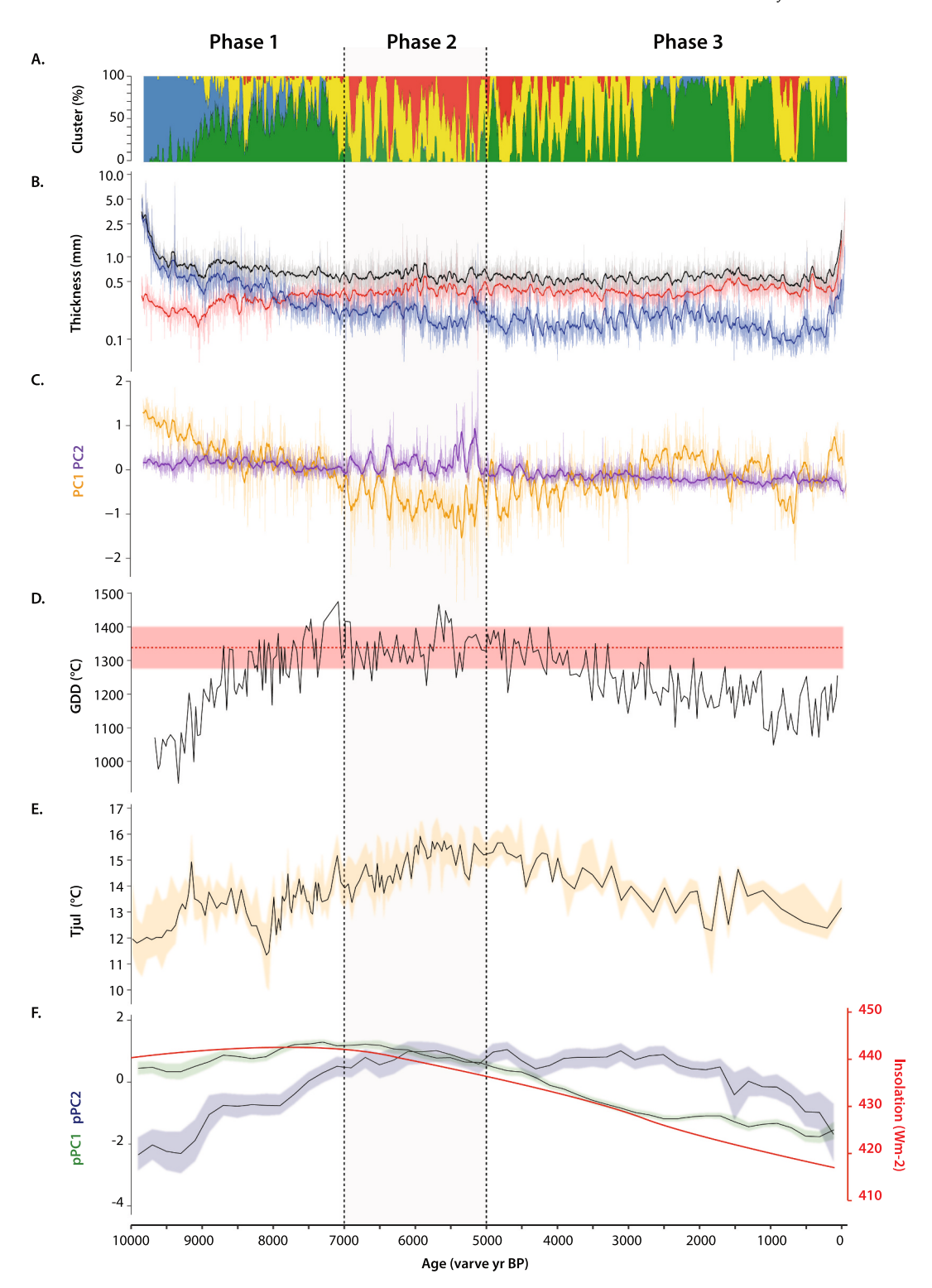


Fig. 5. Comparison of Scandinavian climate records to NAU-23. A. Cumulative area plot from NAU-23 (this study) showing the percentage of cluster occurrences in a 50 yr running window. Cluster colours follow those in Fig. 2. B. Log-scaled Annual (black), Summer (red) and Winter (blue) varve thickness from Nautajärvi (Ojala and Alenius, 2005). Thick lines are 50 year moving averages. C. μ-XRF derived PC1 (yellow) and PC2 (purple) from NAU-23 (this study). D. Pollen-derived growing degree days (GDD >5 °C) from Nautajärvi (Ojala et al., 2008). E. Pollen-based reconstruction of July temperatures using a six-method ensemble from Lake Kuutsjärvi, northern Finland (Salonen et al., 2024). F. Probabilistic principal component 1 (green) and principal component 2 (blue) with 1σ uncertainties of 74 North Atlantic-Fennoscandian sites sensitive to sea surface and continental summer temperature (Sejrup et al., 2016). Phases 1–3 of the NAU-23 sequence are highlighted.

# 6.3. Phase 3- late Holocene (5000 varve yr BP to present)

Phase 3 is characterised by relatively higher detrital influx and a reduction in redox-sensitive element accumulation. The transition

between Phase 2 and 3 at ~5000 varve yr BP broadly coincides with regional reductions in boreal summer temperatures (Ojala et al., 2008; Seppä et al., 2009; Sejrup et al., 2016), and a widespread shift to cooler and wetter conditions in the northerly high European latitudes during

the mid-late Holocene. It has recently been suggested that this transition occurred in close association with a more prominent role of the North Atlantic Oscillation (NAO) in regulating hydroclimatic conditions in southern Scandinavia through to Siberia (Columbu et al., 2023; Czymzik et al., 2023). Lower amplitude variability in PC2, and a reduction in cluster 1 persistence through Phase 3, suggests Fe, Mn and DOM concentrations and hypolimnetic oxidation was consistently lower during the latter stages of the Holocene than during the HTM.

#### 7. Discussion

The HTM stands out in the NAU-23 sequence due to enhanced organic-rich sedimentation, episodic Fe-rich precipitates, and increased variability in PC2. This implies significant changes in lake deposition and mixing regimes occurring in Nautajärvi through the mid-Holocene. The following sections explore how these changes reflect altered lake circulation (section 7.1), a heightened sensitivity of the lake to climatic variability (section 7.2), and the implications for understanding boreal lake responses to future warming (section 7.3).

### 7.1. Lake circulation patterns during the HTM (7000-5000 varve yr BP)

Whilst it is not possible to ascertain the intensity, depth or duration of the seasonal lake circulation cycles, continuous varve preservation means that the hypolimnion remained perennially hypoxic in Nautajärvi, although not permanently anoxic (section 5.2). Clastic-biogenic varves formed continuously during Phases 1 and 3 and are similar to those preserved in the present lake. This suggests that lake circulation was dimictic during both the early and latter stages of the Holocene, with overturn cycles occurring in the spring and autumn months (section 2.1).

Through the HTM (Phase 2) however, the varve sedimentology and  $\mu$ -XRF principal components provide convincing evidence for rapid shifts in varve composition. This can be explained by variations in the lake circulation/stratification regime and hypolimnetic oxidation status which, by implication, could be directly or indirectly climatically controlled.

We argue that the shift to more organic and Fe—Mn rich varves was brought about by a weakened lake circulation regime, with strengthened

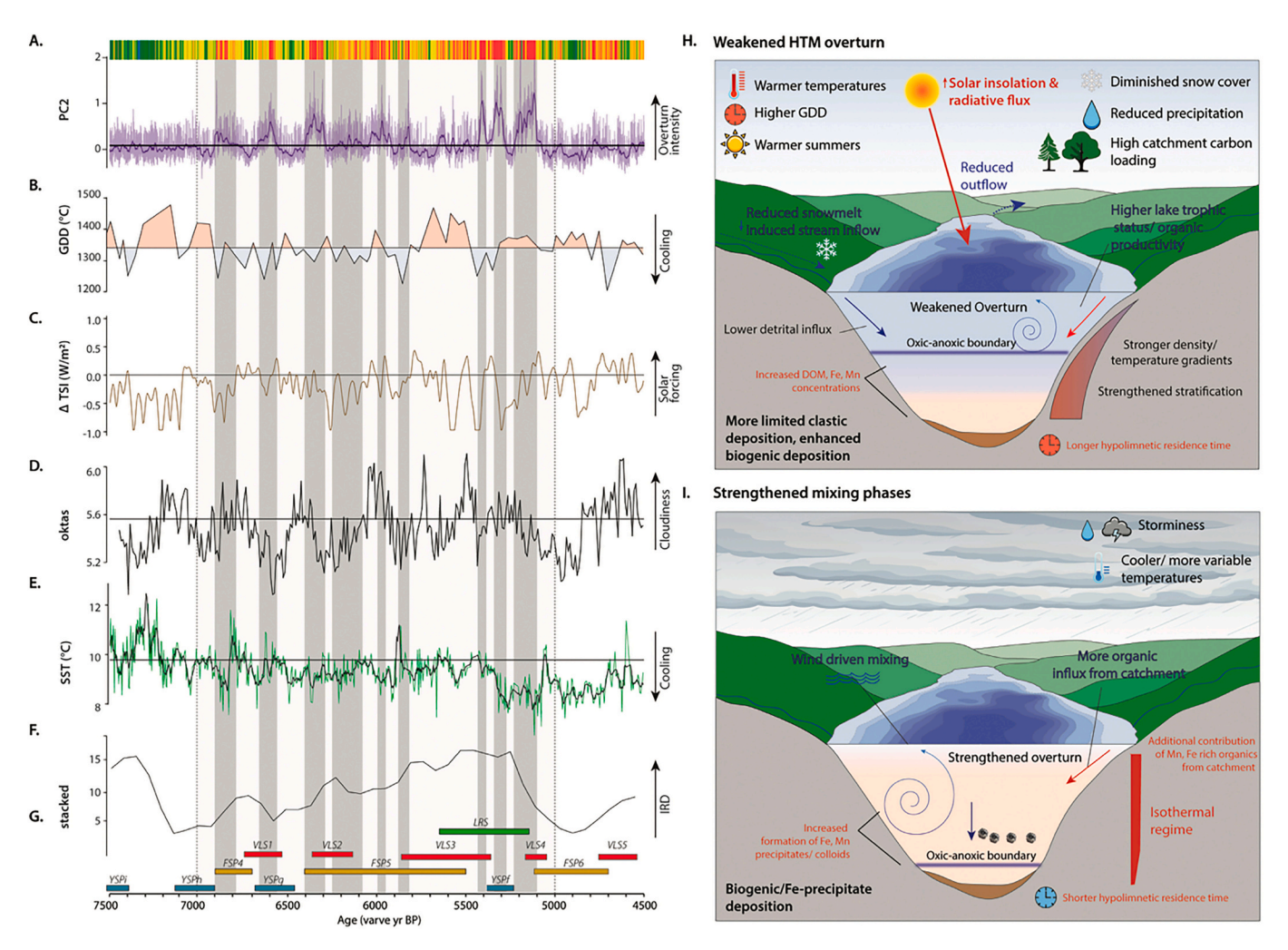


Fig. 6. Regional summary of climatic records from Scandinavia and the North Atlantic between 7500 and 4500 yr BP. A. PC2 values with a 50-yr moving average from Nautajärvi (this study). Cluster results at the top of the figure follow the colours in Fig. 2. B. Palynologically derived GDD >5 °C reconstruction from Nautajärvi (Ojala et al., 2008). Red and blue shading indicates GDD values above and below the 7500-4500 yr BP mean. C. TSI anomalies from Steinhilber et al. (2009). D. Dendrological isotope derived reconstruction of cloud cover and cooling trends in Finnish Lapland (Helama et al., 2021). This curve tracks persistent high atmospheric pressure and the strength of the Siberian high. E. Alkenone derived North Atlantic sea surface temperatures from MD95–2015 in the Iceland Basin. F. Stacked record of the percent hematite-stained grains for North Atlantic marine cores, used to define Bond Events (Bond et al., 2001). G. Records of enhanced Central and Northern European storminess from Yeu, central France (YSPf-i; Pouzet et al., 2018), Filsø in Denmark (FSP4–6; Goslin et al., 2018), Vistula Lagoon, Poland in the southern Baltic Sea (VLS5–1; Uścinowicz et al., 2022), and Lake Ryssjön in southern Sweden (Yu, 2003). H. and I. are schematic illustrations showing processes responsible for weaker HTM lake circulation (H.; light grey) and strengthened mixing phases & ferrogenic deposition associated with the regional cooling and storminess signals (I; dark grey).

and lengthened periods of stratification, and reduced overturning intensity. We conclude that this was driven by three primary mechanisms linked to climatic variability in the HTM, which are summarised in Fig. 6.

First, the thickest biogenic laminae and lowest PC1 values (cluster 1) during the HTM invokes high biological productivity and DOM in the water column, which was promoted by warmer growing seasons (Ojala et al., 2008) and more frequent anticyclonic heatwaves (Antonsson et al., 2008; Mauri et al., 2014; Salminen et al., 2023). The HTM also coincided with regional expansions in deciduous tree cover (Ojala and Alenius, 2005) and peatlands across southern Finland (Korhola, 1995) and western Russia (Novenko et al., 2021), which would further contribute DOM to the lake water via decomposition, soil accumulation and subsequent leaching into the lake's inflowing streams (e.g. Shah et al., 2022). The biogeochemical cycles of Fe, Mn and organic carbon are closely related in lakes, meaning that high DOM concentrations promote the formation of soluble metal complexes including Fe in the water column (Xiao and Riise, 2021). Due to the density of Fe and Mn solutes, these compounds are geochemically focused and become most concentrated in the hypolimnetic waters (e.g. Scholtysik et al., 2020), thereby producing a chemically induced density gradient, which further strengthens lake stratification (Fig. 6).

Second, drier and/or warmer HTM winters would shorten ice cover duration over the lake surface and thereby diminish the strength and length of winter stratification (e.g. Couture et al., 2015). This would shift circulation from a dimictic towards a more monomictic regime (i.e. one overturn cycle per year; Mesman et al., 2021; Woolway and Merchant, 2019). Whilst mild winters would reduce stratification, low catchment snow cover also diminished the strength of the spring overturn, thereby generally reducing the strength of water column circulation and lake through flow. Ultimately, these conditions would lead to a longer residence time of the Fe and Mn enriched hypolimnetic waters.

Third, high concentrations of DOM (as illustrated by low PC1 values and high biogenic laminae thicknesses), and Fe and Mn (as illustrated by high PC2 values and Fe-rich varves) through the HTM would have had significant impacts on lake water transparency. It is well established that high organic and ferric content leads to more opaque surface waters (e.g. Couture et al., 2015; Blanchet et al., 2022), limiting radiative flux to deeper waters, increasing the vertical thermal gradient and reducing the lake mixing depth (e.g. Tichá et al., 2023). Together, these changes are all consistent with weaker, more meromictic circulation (i.e. reduced/more incomplete dimictic overturn intensity through the water column), driven by increased chemical stratification, higher trophic status, and a vertical expansion of the hypoxic hypolimnion through the HTM.

# 7.2. Enhanced lake sensitivity to climatic variability during the HTM

Fe-rich varve preservation in the HTM at 6910–6790, 6660–6560, 6405–6290, 6250–6080,5980–5950, 5850–5810, 5430–5380, 5350–5280 and 5230–5100 varve yr BP, reflects phases of increased Fe precipitate and colloid formation in the water column, under high trophic status and low clastic influx (section 5.2). The accumulation of Fe and Mn precipitates within the varves are interpreted to form in a similar manner to other boreal lakes (e.g. Anthony, 1977; Ballo et al., 2023), with peak accumulation coinciding with the spring and/or autumn overturns via hypolimnetic upwelling and oxidation (Davison, 1993).

We argue that these shifts were driven by intervals of climatic instability (Helama et al., 2021; Sicre et al., 2021; van Dijk et al., 2024; Salonen et al., 2024) and storminess across the European mid-high latitudes (e.g. Yu, 2003; Goslin et al., 2018; Pouzet et al., 2018; Uścinowicz et al., 2022), which impacted circulation and overturn regimes at Nautajärvi, catalysing Fe—Mn and colloidal precipitation in the water column. The most prevalent of these climate anomalies are a series of cooling signals between *ca* 5400 and 5000 yr BP, associated with a cluster of Grand Solar Minima (Steinhilber et al., 2009), reductions in North Atlantic Sea Surface Temperatures (Sicre et al., 2021) and peaks

in ice rafted debris flux (Bond Event 4; Bond et al., 2001). This interval, colloquially termed as the 5.2 ka event (Roland et al., 2015), coincides with the three most distinct increases in PC2 values, iron staining and colloidal precipitation at Nautajärvi, indicating concurrent shifts in varve formation during phases of climatic instability in the HTM (Fig. 6).

We interpret these increases in hypolimnetic oxidation to be a function of intensified lake mixing/ holomixis (Zarczyński et al., 2022; Ballo et al., 2023), during the open water months, in response to regional climatic variability via the following mechanisms.

Cooling and storminess cycles suggest temporarily weaker atmospheric blocking intensities during the spring-autumn months, lowering temperatures, and increasing precipitation and extreme wind speeds across southern Scandinavia (Kautz et al., 2022). These conditions directly enhance lake mixing by: a) weakening thermal stratification (e. g. Jennings et al., 2012; Andersen et al., 2020), b) altering drainage volumes and residence times (e.g. de Eyto et al., 2016); c) increasing lake surface wind shear (e.g. Dräger et al., 2017; Andersen et al., 2020). Cooling and storminess would also impact the lake catchment by: a) increasing winter snow coverage, and the intensity of spring flooding (Ojala and Alenius, 2005); b) enhancing catchment erosion and allogenic organic flux (e.g. Jeppesen et al., 2021). Together, these conditions provide the necessary parameters to enhance DOM, Fe, and Mn concentrations in the lake water (e.g., Klante et al., 2021; Salminen et al., 2023), decrease water stability and lower the redox boundary (Andersen et al., 2020). Under these circumstances, Fe, Mn and colloidal concentrations during the intensified mixing phases would markedly increase, as redox-sensitive ions in the saturated hypolimnetic waters upwell, oxidize and precipitate across the redox boundary (e.g. Woolway et al., 2018; Ballo et al., 2023). We therefore argue that the circulation regime at Nautajärvi repeatedly switched between weaker meromictic and stronger dimictic phases due to climatic instability during the HTM (Fig. 6H-I).

What is notable however, is that the climatic perturbations through the HTM were likely of a lower, and certainly not of a higher magnitude than during earlier and later phases of the Holocene (e.g. the 9.3 ka, 8.2 ka, 4.2 ka, 2.8 ka events and the Little Ice Age), where no comparable variability in lake mixing regime and varve sedimentation is observed. It is clear that iron-rich, colloidal varves only form when lake sedimentation is most strongly dominated by organic material (cluster 1), and lake residence time is sufficiently high to saturate hypolimnetic waters with redox sensitive metal ions. Therefore, the sensitivity of lake mixing to climatic variability is non-stationary, with ferric and manganese precipitate formation occurring only during warmer climatic regimes, when DOM and dissolved Fe and Mn concentrations are high enough to alter the lake's trophic status and stratification regime.

Using the Nautajärvi GDD reconstruction (Ojala et al., 2008), we estimate a threshold at which this increased lake sensitivity is likely to occur. The HTM has a mean GDD of  $1340\pm60~(\sigma)~^{\circ}\text{C}$ , peaking at  $1475~^{\circ}\text{C}$ , which is higher than either Phase 1 ( $1229\pm119~^{\circ}\text{C}$ ), or Phase 3 ( $1230\pm81~^{\circ}\text{C}$ ) (Fig. 5D). Consequently, we suggest that when GDD persistently exceeds ca  $1310~^{\circ}\text{C}$  in southern Scandinavia, the resulting increases in organic and ferric loads in the water column has the potential to alter lake sensitivity to cooling and storminess cycles.

# 7.3. Applicability to future circulation dynamics in boreal lakes

Our investigations demonstrate that climatic variability and associated feedback mechanisms under warmer climatic regimes can have a significant impact on circulation regimes of boreal lakes, even in the absence of anthropogenic interference. The changes observed in the palaeo record can potentially act as an analogue for lake circulation/sedimentation regimes under future warming scenarios in the following ways.

First, future summer seasons are expected to lengthen by between 0.8 and 12.1 days per decade (Woolway, 2023), and summer heatwaves are projected to become longer and more frequent in southern

Scandinavia (Rutgersson et al., 2022). This is a similar pattern to that observed through the HTM, where warmer/ longer summer months (GDD) coincide with higher organic content and a weakened lake circulation regime at Nautajärvi (Ojala et al., 2005). It is likely that summer warming projections will impact small boreal lakes in similar ways, driving alterations in the seasonal timing and duration of lake ice cover, thermal stratification, and weakening circulation (e.g. Couture et al., 2015; Woolway and Merchant, 2019; Jansen et al., 2024).

Second, an increase in DOM, Fe and Mn accumulation in lakes under weakened circulation regimes, is consistent with trends observed in current boreal lake systems undergoing 'brownification' (e.g. Weyhenmeyer et al., 2014; Xiao and Riise, 2021). Lake brownification reduces water opacity and increases temperature-driven density differences in the water column, negatively impacting water quality. Whilst this has been associated with anthropogenic impacts on lakes, the analyses from Nautajärvi show that brownification also occurs naturally in warmer climates, entirely in the absence of major anthropogenic interference. Longer growing seasons and lateral expansions in peatland margins (e.g. Juselius-Rajamäki et al., 2023), are already occurring in southern Fennoscandia, which will only enhance organic loading and future lake brownification without mitigation.

Third, we have identified a non-stationary signal of enhanced lake sensitivity to storminess and cooling intervals under warmer climates with longer/ warmer summers (section 7.2). This is important, as alongside brownification, shifts to colloidal and iron rich sedimentation during these HTM cooling intervals could have a substantial impact on not only the surface drinking water quality (e.g. de Wit et al., 2016; Anderson et al., 2021, 2023), but also on lake ecosystems and food supplies (e.g. Williamson et al., 2015; Woolway, 2023). Climatic perturbations similar in magnitude to the events observed through the HTM, particularly those leading to temporary cooling, will undoubtedly impact future climates in southern Scandinavia. Furthermore, it is likely that the frequency and intensity of Northern European storms will also increase in the future (e.g. Barcikowska et al., 2018; Rutgersson et al., 2022), which, on the basis of this reconstruction, could lead to abrupt and impactful changes in lake mixing regimes and water quality.

Whilst GDD in southern Finland is currently <1200 °C (e.g. Ojala et al., 2008), it is projected to rise and surpass the HTM threshold in the coming decades (Ruosteenoja et al., 2016; Venäläinen et al., 2020). Further work is therefore required on more lakes and quantified palae-otemperature reconstructions, to assess whether the signals observed through the HTM at Nautajärvi represent a more widely applicable threshold of lake sensitivity to seasonally warmer climatic regimes.

### 8. Conclusions

The geochemical composition of the clastic-biogenic varved sediment record from Lake Nautajärvi provides a valuable record of changes in lake circulation regimes through the Holocene. PCA analyses and hierarchical clustering of the  $\mu\textsc{-}XRF$  geochemical data can be used to assess changes in lake sedimentation. PC1 represents shifts in detrital versus organic sedimentation, whilst PC2 reflects non-stationary changes in mixing induced hypolimnetic oxidation.

Three distinct phases of lake sedimentation and circulation are identified through the Holocene. Phase 1 (Early Holocene) was characterised by high detrital input and dimictic circulation, driven by high summer insolation, but cool winter temperatures, extensive ice cover and high spring melt; Phase 2 (HTM) is characterised by increased organic matter and reduced detrital influx, indicating weakened more meromictic circulation, prolonged stratification, and higher biogenic productivity due to warmer and potentially longer summers; Phase 3 (Mid-Late Holocene) shows a return to more clastic-biogenic varve formation, consistent with cooler, wetter conditions and a more stable hypoxic hypolimnion.

During the HTM, the lake experienced heightened sensitivity to temporary cooling intervals and phases of enhanced storminess. These disturbances deepened the lake's mixing regime, increased catchment erosion and organic matter transport, and promoted iron-rich and colloidal varve sedimentation. Heightened sensitivity through the HTM is interpreted to be driven by increased organic and redox element loading, making the hypolimnion less stable to phases of enhanced mixing, promoting lake brownification. These findings suggest that future warming scenarios may lead to similar shifts in the sensitivity of boreal lake mixing regimes to phases of climatic instability.

# CRediT authorship contribution statement

Paul Lincoln: Writing – review & editing, Writing – original draft, Visualization, Investigation, Data curation, Conceptualization. Rik Tjallingii: Writing – review & editing, Methodology, Formal analysis, Data curation. Emilia Kosonen: Writing – review & editing, Investigation. Antti Ojala: Writing – review & editing, Methodology, Investigation, Data curation. Ashley M. Abrook: Writing – review & editing, Investigation, Data curation. Celia Martin-Puertas: Writing – review & editing, Project administration, Investigation, Funding acquisition, Data curation, Conceptualization.

# Declaration of competing interest

The authors declare that they have no known competing financial interests or personal relationships that could have appeared to influence the work reported in this paper.

# Acknowledgements

This study was funded by the UKRI Medical Research Council through a Future Leaders Fellowship held by C.M—P, contributing to the research project DECADAL: Rethinking Palaeoclimatology for Society (MR/W009641/1). The authors wish to thank Saija Saarni who assisted with core extraction from Nautajärvi, and Alice Carter-Champion and Laura Boyall who have engaged in valuable discussions with the authors on lake sedimentation processes, XRF analyses and the final code structure included in the supplementary information.

# Appendix A. Supplementary data

Supplementary data to this article can be found online at  $\frac{\text{https:}}{\text{doi.}}$  org/10.1016/j.scitotenv.2025.178519.

# Data availability

The NAU-23  $\mu\text{-XRF}$  data are available on Zenodo: https://doi.org/10.5281/zenodo.14645779 and the varve thickness data are available on Pangaea: https://doi.org/10.1594/PANGAEA.968802. R code used to run the analyses is included in the supplementary data.

# References

Aitchison, J., 1986. The Statistical Analysis of Compositional Data. Chapman & Hall. Algeo, T.J., Li, C., 2020. Redox classification and calibration of redox thresholds in sedimentary systems. Geochim. Cosmochim. Acta 287, 8–26. https://doi.org/ 10.1016/j.gca.2020.01.055.

Andersen, M.R., de Eyto, E., Dillane, M., Poole, R., Jennings, E., 2020. 13 years of storms: an analysis of the effects of storms on lake physics on the Atlantic fringe of Europe. Water 12 (2), 318.

Anderson, L.E., DeMont, I., Dunnington, D.D., Bjorndahl, P., Redden, D.J., Brophy, M.J., Gagnon, G.A., 2023. A review of long-term change in surface water natural organic matter concentration in the northern hemisphere and the implications for drinking water treatment. Sci. Total Environ. 858, 159699. https://doi.org/10.1016/j. scitotenv.2022.159699.

Anderson, L.E., Trueman, B.F., Dunnington, D.W., Gagnon, G.A., 2021. Relative importance of organic- and iron-based colloids in six Nova Scotian lakes. Npj clean. Water 4, 1–10. https://doi.org/10.1038/s41545-021-00115-4.

Anthony, R.S., 1977. Iron-rich rhythmically laminated sediments in Lake of the clouds, northeastern Minnesotal. Limnol. Oceanogr. 22, 45–54. https://doi.org/10.4319/ lo.1977.22.1.0045.

- Antonsson, K., Chen, D., Seppa, H., 2008. Anticyclonic Atmospheric Circulation as an Analogue for the Warm and Dry Mid-Holocene Summer Climate in Central Scandinavia. Clim, Past.
- Ballo, E.G., Bajard, M., Støren, E., Bakke, J., 2023. Using microcomputed tomography (µCT) to count varves in Lake sediment sequences: application to Lake Sagtjernet. Eastern Norway. Quaternary Geochronology 75, 101432. https://doi.org/10.1016/j.guageo.2023.101432.
- Barcikowska, M.J., Weaver, S.J., Feser, F., Russo, S., Schenk, F., Stone, D.A., Wehner, M. F., Zahn, M., 2018. Euro-Atlantic winter storminess and precipitation extremes under 1.5 °C vs. 2 °C warming scenarios. Earth Syst. Dynam. 9, 679–699. https://doi.org/10.5194/esd-9-679-2018.
- Bertrand, S., Tjallingii, R., Kylander, M., et al., 2023. Inorganic geochemistry of lake sediments: a review of analytical techniques and guidelines for interpretation. Earth Sci. Rev. 249, 104639. https://doi.org/10.1016/j.earscirev.2023.104639.
- Blanchet, C.C., Arzel, C., Davranche, A., Kahilainen, K.K., Secondi, J., Taipale, S., Lindberg, H., Loehr, J., Manninen-Johansen, S., Sundell, J., Maanan, M., Nummi, P., 2022. Ecology and extent of freshwater browning - what we know and what should be studied next in the context of global change. Sci. Total Environ. 812, 152420. https://doi.org/10.1016/j.scitotenv.2021.152420.
- Bond, G., Kromer, B., Beer, J., Muscheler, R., Evans, M.N., Showers, W., Hoffmann, S., Lotti-Bond, R., Hajdas, I., Bonani, G., 2001. Persistent solar influence on North Atlantic climate during the Holocene. Science 294, 2130–2136. https://doi.org/ 10.1126/science.1065680.
- Borzenkova, I., Zorita, E., Borisova, O., Kalniņa, L., Kisielienė, D., Koff, T., Kuznetsov, D., Lemdahl, G., Sapelko, T., Stančikaitė, M., Subetto, D., 2015. Climate change during the Holocene (past 12,000 years). Second assessment of climate change for the Baltic Sea basin 25–49.
- Bova, S., Rosenthal, Y., Liu, Z., Godad, S.P., Yan, M., 2021. Seasonal origin of the thermal maxima at the Holocene and the last interglacial. Nature 589 (7843), 548–553.
- Charrad, Malika, Ghazzali, Nadia, Boiteau, Véronique, Niknafs, Azam, 2014. NbClust: an R package for determining the relevant number of clusters in a data set. J. Stat. Softw. 61 (November), 1–36. https://doi.org/10.18637/jss.v061.i06.
- Columbu, A., Zhornyak, L.V., Zanchetta, G., Drysdale, R.N., Hellstrom, J.C., Isola, I., Regattieri, E., Fallick, A.E., 2023. A mid-Holocene stalagmite multiproxy record from southern Siberia (Krasnoyarsk, Russia) linked to the Siberian high patterns. Quat. Sci. Rev. 320, 108355. https://doi.org/10.1016/j.quascirev.2023.108355.
- Couture, R.M., de Wit, H.A., Tominaga, K., Kiuru, P., Markelov, I., 2015. Oxygen dynamics in a boreal lake responds to long-term changes in climate, ice phenology, and DOC inputs. J. Geophys. Res. Biogeosci. 120 (11), 2441–2456. https://doi.org/10.1002/2015JG003065.
- Czymzik, M., Tjallingii, R., Plessen, B., Feldens, P., Theuerkauf, M., Moros, M., Schwab, M.J., Nantke, C.K.M., Pinkerneil, S., Brauer, A., Arz, H.W., 2023. Mid-Holocene reinforcement of North Atlantic atmospheric circulation variability from a western Baltic lake sediment record. Clim. Past 19, 233–248. https://doi.org/10.5194/cp-19-233-2023.
- Davison, W., 1993. Iron and manganese in lakes. Earth Sci. Rev. 34 (2), 119–163. https://doi.org/10.1016/0012-8252(93)90029-7.
- Davison, W., Woof, C., Rigg, E., 1982. The dynamics of Iron and manganese in a seasonally anoxic Lake; direct measurement of fluxes using sediment traps. Limnol. Oceanogr. 27, 987–1003.
- de Eyto, E., Jennings, E., Ryder, E., Sparber, K., Dillane, M., Dalton, C., Poole, R., 2016. Response of a humic lake ecosystem to an extreme precipitation event: physical, chemical, and biological implications. Inland Waters 6 (4), 483–498.
- de Wit, H.A., Valinia, S., Weyhenmeyer, G.A., Futter, M.N., Kortelainen, P., Austnes, K., Hessen, D.O., Räike, A., Laudon, H., Vuorenmaa, J., 2016. Current Browning of surface waters will be further promoted by wetter climate. Environ. Sci. Technol. Lett. 3, 430–435. https://doi.org/10.1021/acs.estlett.6b00396.
- Dräger, N., Theuerkauf, M., Szeroczyńska, K., Wulf, S., Tjallingii, R., Plessen, B., Kienel, U., Brauer, A., 2017. Varve microfacies and varve preservation record of climate change and human impact for the last 6000 years at Lake Tiefer see (NE Germany). The Holocene 27 (3), 450–464. https://doi.org/10.1177/0959683616660173.
- Engels, S., 2021. The influence of Holocene forest dynamics on the chironomid fauna of a boreal lake (Flocktjärn, Northeast Sweden). Boreas 50, 519–534. https://doi.org/ 10.1111/bor.12497.
- Galili, T., 2015. Dendextend: an R package for visualizing, adjusting and comparing trees of hierarchical clustering. Bioinformatics 31 (22), 3718–3720.
- Gälman, V., Rydberg, J., Shchukarev, A., Sjöberg, S., Martínez-Cortizas, A., Bindler, R., Renberg, I., 2009. The role of iron and sulfur in the visual appearance of lake sediment varves. J. Paleolimnol. 42, 141–153. https://doi.org/10.1007/s10933-008-9267-6.
- Goslin, J., Fruergaard, M., Sander, L., Gałka, M., Menviel, L., Monkenbusch, J., Thibault, N., Clemmensen, L.B., 2018. Holocene centennial to millennial shifts in North-Atlantic storminess and ocean dynamics. Sci. Rep. 8, 12778. https://doi.org/ 10.1038/s41598-018-29949-8.
- Gu, Z., Hübschmann, D., 2022. Make interactive complex heatmaps in R. Bioinformatics 38 (5), 1460–1462. https://doi.org/10.1093/bioinformatics/btab806.
- Haltia-Hovi, E., Saarinen, T., Kukkonen, M., 2007. A 2000-year record of solar forcing on varved lake sediment in eastern Finland. Quat. Sci. Rev. 26, 678–689. https://doi. org/10.1016/j.quascirev.2006.11.005.
- Heikkilä, M., Seppä, H., 2003. A 11,000 yr palaeotemperature reconstruction from the southern boreal zone in Finland. Quat. Sci. Rev. 22 (5–7), 541–554.
- Helama, S., Stoffel, M., Hall, R.J., Jones, P.D., Arppe, L., Matskovsky, V.V., Timonen, M., Nöjd, P., Mielikäinen, K., Oinonen, M., 2021. Recurrent transitions to little ice agelike climatic regimes over the Holocene. Clim. Dyn. 56, 3817–3833. https://doi.org/ 10.1007/s00382-021-05669-0.

- Jansen, J., Simpson, G.L., Weyhenmeyer, G.A., et al., 2024. Climate-driven deoxygenation of northern lakes. Nat. Clim. Chang. 14, 832–838. https://doi.org/ 10.1038/s41558-024-02058-3.
- Jennings, E., Jones, S., Arvola, L., Staehr, P.A., Gaiser, E., Jones, I.D., Weathers, K.C., Weyhenmeyer, G.A., CHIU, C.Y. and De Eyto, E., 2012. Effects of weather-related episodic events in lakes: an analysis based on high-frequency data. Freshw. Biol. 57 (3), 589–601.
- Jeppesen, E., Pierson, D., Jennings, E., 2021. Effect of extreme climate events on lake ecosystems. Water 13 (3), 282.
- Jokinen, P., Pirinen, P., Kaukoranta, J.-P., Kangas, A., Alenius, P., Eriksson, P., Johansson, M., Wilkman, S., 2021. Climatological and oceanographic statistics of Finland 1991–2020. Finnish Meteorological Institute, Reports 2021, 8, p. 196.
- Juselius-Rajamäki, T., Väliranta, M., Korhola, A., 2023. The ongoing lateral expansion of peatlands in Finland. Glob. Chang. Biol. 29, 7173–7191. https://doi.org/10.1111/ gcb.16988.
- Kassambara, A., Mundt, F., 2017. Package 'factoextra'. Extract and visualize the results of multivariate data analyses 76 (2).
- Kautz, L.A., Martius, O., Pfahl, S., Pinto, J.G., Ramos, A.M., Sousa, P.M., Woollings, T., 2022. Atmospheric blocking and weather extremes over the euro-Atlantic sector—a review. Weather and climate dynamics 3 (1), 305–336.
- Klante, C., Larson, M., Persson, K.M., 2021. Brownification in Lake Bolmen, Sweden, and its relationship to natural and human-induced changes. Journal of Hydrology: Regional Studies 36, 100863. https://doi.org/10.1016/j.eirh.2021.100863.
- Knoll, L.B., Williamson, C.E., Pilla, R.M., Leach, T.H., Brentrup, J.A., Fisher, T.J., 2018. Browning-related oxygen depletion in an oligotrophic lake. Inland Waters 8, 255–263. https://doi.org/10.1080/20442041.2018.1452355.
- Korhola, A., 1995. Holocene climatic variations in southern Finland reconstructed from peat-initiation data. The Holocene 5, 43–57. https://doi.org/10.1177/ 095968369500500106.
- Korkonen, S.T., Ojala, A.E.K., Kosonen, E., Weckström, J., 2017. Seasonality of Chrysophyte cyst and diatom assemblages in Varved Lake Nautajärvi – implications for Palaeolimnological studies. J. Limnol. 76 (2). https://doi.org/10.4081/ ilimnol.2017.1473.
- Krzeminski, P., Vogelsang, C., Meyn, T., Köhler, S.J., Poutanen, H., de Wit, H.A., Uhl, W., 2019. Natural organic matter fractions and their removal in full-scale drinking water treatment under cold climate conditions in Nordic capitals. J. Environ. Manag. 241, 427–438. https://doi.org/10.1016/j.jenvman.2019.02.024.
- Lê, S., Josse, J., Husson, F., 2008. FactoMineR: an R package for multivariate analysis. J. Stat. Softw. 25, 1–18.
- Luo, Y., 2018, July. Geochemical cycle and environmental effects of sulfur in lakes. In: IOP Conference Series: Materials Science and Engineering, vol. 394, No. 5. IOP Publishing, 052039.
- Makri, S., Wienhues, G., Bigalke, M., Gilli, A., Rey, F., Tinner, W., Vogel, H., Grosjean, M., 2021. Variations of sedimentary Fe and Mn fractions under changing lake mixing regimes, oxygenation and land surface processes during late-glacial and Holocene times. Sci. Total Environ. 755, 143418. https://doi.org/10.1016/j. scitotenv.2020.143418.
- Mauri, A., Davis, B.a.S., Collins, P.M., Kaplan, J.O., 2014. The influence of atmospheric circulation on the mid-Holocene climate of Europe: a data—model comparison. Clim. Past 10, 1925–1938. https://doi.org/10.5194/cp-10-1925-2014.
- Mesman, J.P., Stelzer, J.A., Dakos, V., Goyette, S., Jones, I.D., Kasparian, J., McGinnis, D. F., Ibelings, B.W., 2021. The role of internal feedbacks in shifting deep lake mixing regimes under a warming climate. Freshw. Biol. 66 (6), 1021–1035.
- Mishra, P.K., 2023. Lake sediments and climate studies. In: The Application of Lake Sediments for Climate Studies. SpringerBriefs in Environmental Science. Springer, Cham. https://doi.org/10.1007/978-3-031-34709-2\_1.
- Naeher, S., Gilli, A., North, R.P., Hamann, Y., Schubert, C.J., 2013. Tracing bottom water oxygenation with sedimentary Mn/Fe ratios in Lake Zurich, Switzerland. Chem. Geol. 352, 125–133. https://doi.org/10.1016/j.chemgeo.2013.06.006.
- Neugebauer, I., Thomas, C., Ordoñez, L., Waldmann, N.D., Recasens, C., Vizcaino, A., Jimenez-Espejo, F.J., Ariztegui, D., 2022. Preservation of Fe/Mn-redox fronts in sediments of an oligotrophic, oxygenated deep-water lake (Lago Fagnano, Tierra del Fuego). Sedimentology 69, 1841–1860. https://doi.org/10.1111/sed.12976.
- Novenko, E.Y., Mazei, N.G., Kupriyanov, D.A., Kusilman, M.V., Olchev, A.V., 2021. Peatland initiation in central European Russia during the Holocene: effect of climate conditions and fires. The Holocene 31, 545–555. https://doi.org/10.1177/ 0959683620981709.
- Ojala, A., Saarinen, T., Salonen, V.-P., 2000. Preconditions for the formation of annually laminated lake sediments in southern and Central Finland. Boreal Environ. Res. 5, 243-255
- Ojala, A.E., Alenius, T., Seppä, H., Giesecke, T., 2008. Integrated varve and pollen-based temperature reconstruction from Finland: evidence for Holocene seasonal temperature patterns at high latitudes. The Holocene 18 (4), 529–538.
- Ojala, A.E., Kosonen, E., Weckström, J., Korkonen, S., Korhola, A., 2013. Seasonal formation of clastic-biogenic varves: the potential for palaeoenvironmental interpretations. GFF 135 (3–4), 237–247.
- Ojala, A.E., Tiljander, M., 2003. Testing the fidelity of sediment chronology: comparison of varve and paleomagnetic results from Holocene lake sediments from Central Finland. Quat. Sci. Rev. 22 (15–17), 1787–1803. https://doi.org/10.1016/S0277-3791(03)00140-9.
- Ojala, A.E.K., Alenius, T., 2005. 10000 years of interannual sedimentation recorded in the Lake Nautajärvi (Finland) clastic-organic varves. Palaeogeogr. Palaeoclimatol. Palaeoecol. 219, 285–302. https://doi.org/10.1016/j.palaeo.2005.01.002.
- Ojala, A.E.K., Francus, P., 2002. Comparing X-ray densitometry and BSE-image analysis of thin section in varved sediments. Boreas 31 (1), 57–64.

- Ojala, A.E.K., Heinsalu, A., Saarnisto, M., Tiljander, M., 2005. Annually laminated sediments date the drainage of the Ancylus Lake and early Holocene shoreline displacement in Central Finland. Quaternary International, Baltic Sea Science Congress 2001 (130), 63–73. https://doi.org/10.1016/j.quaint.2004.04.032.
- Pouzet, P., Maanan, M., Piotrowska, N., Baltzer, A., Stéphan, P., Robin, M., 2018. Chronology of Holocene storm events along the European Atlantic coast: new data from the island of Yeu, France. Progress in Physical Geography: Earth and Environment 42, 431–450. https://doi.org/10.1177/0309133318776500.
- Renberg, I., 1981. Formation, structure and visual appearance of iron-rich, varved lake sediments. SIL Proceedings 1922-2010 (21), 94–101. https://doi.org/10.1080/ 03680770.1980.11896963.
- Riise, G., Haaland, S.L., Xiao, Y., 2023. Coupling of iron and dissolved organic matter in lakes–selective retention of different size fractions. Aquat. Sci. 85, 57. https://doi. org/10.1007/s00027-023-00956-w.
- Roland, T.P., Daley, T.J., Caseldine, C.J., Charman, D.J., Turney, C.S.M., Amesbury, M.J., Thompson, G.J., Woodley, E.J., 2015. The 5.2 ka climate event: evidence from stable isotope and multi-proxy palaeoecological peatland records in Ireland. Quat. Sci. Rev. 124, 209–223. https://doi.org/10.1016/j.quascirev.2015.07.026.
- Ruosteenoja, K., Räisänen, J., Venäläinen, A., Kämäräinen, M., 2016. Projections for the duration and degree days of the thermal growing season in Europe derived from CMIP5 model output. Int. J. Climatol. 36 (8). https://doi.org/10.1002/joc.4535.
- Rutgersson, A., Kjellström, E., Haapala, J., Stendel, M., Danilovich, I., Drews, M., Jylhä, K., Kujala, P., Larsén, X.G., Halsnæs, K., Lehtonen, I., 2022. Natural hazards and extreme events in the Baltic Sea region. Earth Syst. Dynam. 13 (1), 251–301. https://doi.org/10.5194/esd-13-251-2022.
- Saarni, S., Muschitiello, F., Weege, S., Brauer, A., Saarinen, T., 2016. A late Holocene record of solar-forced atmospheric blocking variability over Northern Europe inferred from varved lake sediments of Kuninkaisenlampi. Quat. Sci. Rev. 154, 100–110. https://doi.org/10.1016/j.quascirev.2016.10.019.
- Salminen, S., Saarni, S., Saarinen, T., 2023. Sensitivity of varve biogenic component to climate in eastern and Central Finland. J. Paleolimnol. 70 (2), 113–130. https://doi. org/10.1007/s10933-023-00287-8.
- Salminen, S., Saarni, S., Tammelin, M., Fukumoto, Y., Saarinen, T., 2019. Varve distribution reveals spatiotemporal Hypolimnetic hypoxia oscillations during the past 200 years in Lake Lehmilampi. Eastern Finland. Quaternary 2, 20. https://doi. org/10.3390/guat2020020.
- Salonen, J.S., Kuosmanen, N., Alsos, I.G., Heintzman, P.D., Rijal, D.P., Schenk, F., Bogren, F., Luoto, M., Philip, A., Piilo, S., Trasune, L., Väliranta, M., Helmens, K.F., 2024. Uncovering Holocene climate fluctuations and ancient conifer populations: insights from a high-resolution multi-proxy record from northern Finland. Glob. Planet. Chang. 237. 104462. https://doi.org/10.1016/j.gloplacha.2024.104462.
- Sarkkola, S., Nieminen, M., Koivusalo, H., Laurén, A., Kortelainen, P., Mattsson, T., Palviainen, M., Piirainen, S., Starr, M., Finér, L., 2013. Iron concentrations are increasing in surface waters from forested headwater catchments in eastern Finland. Sci. Total Environ. 463–464, 683–689. https://doi.org/10.1016/j. scitotenv.2013.06.072.
- Scholtysik, G., Dellwig, O., Roeser, P., Arz, H.W., Casper, P., Herzog, C., Goldhammer, T., Hupfer, M., 2020. Geochemical focusing and sequestration of manganese during eutrophication of Lake Stechlin (NE Germany). Biogeochemistry 151 (2), 313–334. https://doi.org/10.1007/s10533-020-00729-9.
- Sejrup, H.P., Seppä, H., McKay, N.P., Kaufman, D.S., Geirsdóttir, Á., de Vernal, A., Renssen, H., Husum, K., Jennings, A., Andrews, J.T., 2016. Quat. Sci. Rev. 147, 365–378. https://doi.org/10.1016/j.quascirev.2016.06.005. Special Issue: PAST Gateways (Palaeo-Arctic Spatial and Temporal Gateways).
- Seppä, H., Bjune, A.E., Telford, R.J., Birks, H.J.B., Veski, S., 2009. Last nine-thousand years of temperature variability in northern Europe. Clim. Past 5, 523–535. https:// doi.org/10.5194/cp-5-523-2009.
- Shah, N.W., Baillie, B.R., Bishop, K., Ferraz, S., Högbom, L., Nettles, J., 2022. The effects of forest management on water quality. For. Ecol. Manag. 522, 120397. https://doi.org/10.1016/j.foreco.2022.120397.
- Shatwell, T., Thiery, W., Kirillin, G., 2019. Future projections of temperature and mixing regime of European temperate lakes. Hydrol. Earth Syst. Sci. 23, 1533–1551. https://doi.org/10.5194/hess-23-1533-2019.
- Sicre, M.-A., Jalali, B., Eiríksson, J., Knudsen, K.-L., Klein, V., Pellichero, V., 2021. Trends and centennial-scale variability of surface water temperatures in the North Atlantic during the Holocene. Quat. Sci. Rev. 265, 107033. https://doi.org/10.1016/j. guascirev.2021.107033.
- Snowball, I., Zillén, L., Ojala, A., Saarinen, T., Sandgren, P., 2007. FENNOSTACK and FENNORPIS: varve dated Holocene palaeomagnetic secular variation and relative palaeointensity stacks for Fennoscandia. Earth Planet. Sci. Lett. 255 (1–2), 106–116. https://doi.org/10.1016/j.epsl.2006.12.009.
- Steinhilber, F., Beer, J., Fröhlich, C., 2009. Total solar irradiance during the Holocene. Geophys. Res. Lett. 36 (19). https://doi.org/10.1029/2009GL040142.
- Taipale, S.J., Vuorio, K., Strandberg, U., Kahilainen, K.K., Järvinen, M., Hiltunen, M., Peltomaa, E., Kankaala, P., 2016. Lake eutrophication and brownification downgrade availability and transfer of essential fatty acids for human consumption. Environ. Int. 96, 156–166. https://doi.org/10.1016/j.envint.2016.08.018.
- Tichá, A., Vondrák, D., Moravcová, A., Chiverrell, R., Kuneš, P., 2023. Climate-related soil saturation and peatland development may have conditioned surface water

- brownification at a central European lake for millennia. Sci. Total Environ. 858, 159982. https://doi.org/10.1016/j.scitotenv.2022.159982.
- Tiljander, M., Ojala, A., Saarinen, T., Snowball, I., 2002. Documentation of the physical properties of annually laminated (varved) sediments at a sub-annual to decadal resolution for environmental interpretation. Quat. Int. 88 (1), 5–12.
- Tiljander, M., Saarnisto, M., Ojala, A.E.K., Saarinen, T., 2003. A 3000-year palaeoenvironmental record from annually laminated sediment of Lake Korttajarvi, Central Finland. Boreas 32, 566–577. https://doi.org/10.1111/j.1502-3885.2003. tb01236.x.
- Tjallingii, R., Röhl, U., Kölling, M., et al., 2007. Influence of the water content on X-ray fluorescence core-scanning measurements in soft marine sediments. Geochem. Geophys. Geosyst. 8. https://doi.org/10.1029/2006GC001393.
- Uścinowicz, S., Cieślikiewicz, W., Skrzypek, G., Zgrundo, A., Goslar, T., Jędrysek, M.-O., Jurys, L., Koszka-Maroń, D., Miotk-Szpiganowicz, G., Sydor, P., Zachowicz, J., 2022. Holocene relative water level and storminess variation recorded in the coastal peat bogs of the Vistula lagoon, southern Baltic Sea. Quat. Sci. Rev. 296, 107782. https://doi.org/10.1016/j.quascirev.2022.107782.
- Van den Boogaart, K.G., Tolosana-Delgado, R., 2008. "Compositions": a unified R package to analyze compositional data. Comput. Geosci. 34 (4), 320–338.
- Van Dijk, E.J.C., Jungclaus, J., Sigl, M., Timmreck, C., Krüger, K., 2024. High-frequency climate forcing causes prolonged cold periods in the Holocene. Commun Earth Environ 5, 242. https://doi.org/10.1038/s43247-024-01380-0.
- Veijalainen, N., Ahopelto, L., Marttunen, M., Jääskeläinen, J., Britschgi, R., Orvomaa, M., Belinskij, A., Keskinen, M., 2019. Severe drought in Finland: modeling effects on water resources and assessing climate change impacts. Sustainability 11 (8), 2450.
- Venäläinen, A., Lehtonen, I., Laapas, M., Ruosteenoja, K., Tikkanen, O.-P., Viiri, H., Ikonen, V.-P., Peltola, H., 2020. Climate change induces multiple risks to boreal forests and forestry in Finland: a literature review. Glob. Chang. Biol. 26, 4178–4196. https://doi.org/10.1111/gcb.15183.
- Wastegård, S., 2022. The Holocene of Sweden a review. GFF 144, 126–149. https://doi. org/10.1080/11035897.2022.2086290.
- Wei, T., Simko, V., Levy, M., Xie, Y., Jin, Y., Zemla, J., 2017. Package 'corrplot'. Statistician 56 (316), e24.
- Weltje, C.J., Bloemsma, M.R., Tjallingii, R., et al., 2015. Prediction of geochemical composition from XRF Core scanner data: A new multivariate approach including automatic selection of calibration samples and quantification of uncertainties. In: Croudace, I.W., Rothwell, R.G. (Eds.), Micro-XRF Studies of Sediment Cores: Applications of a Non-Destructive Tool for the Environmental Sciences, Developments in Paleoenvironmental Research. Springer, Netherlands, Dordrecht, pp. 507–534. https://doi.org/10.1007/978-94-017-9849-5 21.
- Weltje, G.J., Tjallingii, R., 2008. Calibration of XRF core scanners for quantitative geochemical logging of sediment cores: theory and application. Earth Planet. Sci. Lett. 274 (3–4), 423–438. https://doi.org/10.1016/j.epsl.2008.07.054.
- Wetzel, Robert G., 2001. Limnology: lake and river ecosystems. gulf professional publishing.
- Weyhenmeyer, G.A., Prairie, Y.T., Tranvik, L.J., 2014. Browning of boreal freshwaters coupled to carbon-iron interactions along the aquatic continuum. PLoS One 9 (2), e88104.
- Wickham, H., 2016. ggplot2: elegant graphics for data analysis.
- Williamson, C.E., Overholt, E.P., Pilla, R.M., Leach, T.H., Brentrup, J.A., Knoll, L.B., Mette, E.M., Moeller, R.E., 2015. Ecological consequences of long-term browning in lakes. Sci. Rep. 5, 18666. https://doi.org/10.1038/srep18666.
- Woolway, R.I., 2023. The pace of shifting seasons in lakes. Nat. Commun. 14, 2101. https://doi.org/10.1038/s41467-023-37810-4.
- Woolway, R.I., Merchant, C.J., 2019. Worldwide alteration of lake mixing regimes in response to climate change. Nat. Geosci. 12, 271–276. https://doi.org/10.1038/ s41561-019-0322-x.
- Woolway, R.I., Simpson, J.H., Spiby, D., Feuchtmayr, H., Powell, B., Maberly, S.C., 2018. Physical and chemical impacts of a major storm on a temperate lake: a taste of things to come? Clim. Chang. 151, 333–347.
- Xiao, Y., Riise, G., 2021. Coupling between increased lake color and iron in boreal lakes. Sci. Total Environ. 767, 145104. https://doi.org/10.1016/j.scitotenv.2021.145104.
- Yu, S.-Y., 2003. Centennial-scale cycles in middle Holocene Sea level along the southeastern Swedish Baltic coast. Geo. Society Am. Bull. 115, 1404. https://doi. org/10.1130/B25217.1.
- Żarczyński, M., Wacnik, A., Tylmann, W., 2019. Tracing lake mixing and oxygenation regime using the Fe/Mn ratio in varved sediments: 2000 year-long record of humaninduced changes from Lake Żabińskie (NE Poland). Sci. Total Environ. 657, 585–596. https://doi.org/10.1016/j.scitotenv.2018.12.078.
- Zarczyński, M., Zander, P.D., Grosjean, M., Tylmann, W., 2022. Linking the formation of varves in a eutrophic temperate lake to meteorological conditions and water column dynamics. Sci. Total Environ. 842, 156787.
- Zeileis, A., Grothendieck, G., Ryan, J.A., Andrews, F., Zeileis, M.A., 2023. Package 'zoo'. R package version 1–7.
- Zolitschka, B., Francus, P., Ojala, A.E.K., Schimmelmann, A., 2015. Varves in lake sediments – a review. Quat. Sci. Rev. 117, 1–41. https://doi.org/10.1016/j. quascirev.2015.03.019.